Analysis of SUMO dynamics and functions during meiosis in oocytes

Ding Yi

Table of Contents

Abstract

In meiosis, haploid gametes are produced through two successive cell divisions with only one round of chromosome replication. In meiosis I, homologous chromosomes are physically held together by chiasmata, which are supported by cohesion along the chromosome arm. Chromosome cohesion is mediated by the cohesin complex and determines the specific segregation pattern of chromosomes in meiosis. At anaphase I onset, the protease separase cleaves cohesin along the chromosome arm, and thus homologous chromosomes are separated into opposite sides. However, centromeric cohesin is protected from the cleavage and keeps sister chromosomes together until metaphase II. It has been shown that shugoshin Sgo2 is recruited to centromeres in meiosis and antagonizes separase activity at anaphase I onset. However, it remains unclear how centromeric cohesion is protected during late anaphase I and telophase I, in which Sgo2 is undetectable. Here, in this study, I found that the SUMO E3 ligase PIAS proteins and SUMO2/3 are enriched near centromeres at telophase I in mouse oocytes. If a centromere-targeted dominant-negative form of PIAS1 is expressed, enrichment of centromeric SUMO2/3 is inhibited. These oocytes undergo precocious sister chromatid separation due to loss of centromeric cohesin by metaphase II, while they are proficient in Sgo2-dependent cohesion protection at anaphase I onset. Artificial cleavage of the centromere-targeted dominant-negative PIAS1 at anaphase I onset rescues the centromeric SUMO2/3 enrichment at telophase I and alleviates precocious chromosome separation at metaphase II. In summary, post-anaphase-I sumoylation enrichment is required for centromeric cohesion maintenance during meiosis I-II transition in mouse oocytes.

Abbreviation

SUMO: small ubiquitin-related modifier

Y2H: yeast two hybrid

CDS: coding DNA sequence

SAC: spindle assembly checkpoint

Sgo: Shugoshin

GVBD: germinal vesicle breakdown

PMSG: pregnant mare serum gonadotropin

HCG: Human chorionic gonadotropin

IBMX: 3-isobutyl-1-methylxanthine

SMC protein: structural maintenance of chromosomes protein

APC/C: anaphase promoting complex/cyclosome

Wapl: Wings apart-like protein homolog, chromosome partitioning

PFA: paraformaldehyde

DMSO: Dimethyl sulfoxide

PEG: polyethylene glycol

MEIKIN: meiosis-specific kinetochore protein

SPF: specific pathogen-free

1. Introduction

Cell division is a key event responsible for development, growth, maintenance and reproduction of biosystems. During cell division, a parent cell divides into two daughter cells. How to transmit genetic information to daughter cells is a fundamental task for organisms. In eukaryotes, organisms have evolved two types of cell division to fulfill two different missions, mitosis and meiosis. Mitosis is responsible for development, growth and maintenance, while meiosis is responsible for reproduction. In either case, parent cells only duplicate genome DNA once. Cells that undergo mitosis have to divide duplicated chromosomes equally so that daughter cells receive exactly the same genome from the parent cell. In contrast, cells that undergo meiosis have to separate chromosomes twice, resulting in a halved genome. In the first division of meiosis (meiosis I), homologous chromosomes from the mother and father are separated and segregated into daughter cells, while sister chromatids are held together until the second division of meiosis. In the second division, sister chromatids are segregated into daughter cells, which thus results in the production of haploid gametes. Faithful segregation of chromosomes in meiosis is essential for producing healthy gametes. Fertilization of aneuploid gametes leads to compromised embryonic development and congenital disease.

In mitosis, the “search and capture” model is widely accepted to explain the equal partition of sister chromatids. In this model, paired sister kinetochores are captured and pulled by microtubule bundles emanating from two spindle poles. Cohesions between sister kinetochores counteract the forces generated by microtubule bundles from

opposite spindle poles. When the forces are balanced, the sister chromatids becomes bi-oriented at the equator of the spindle (Fig. 1), which is a prerequisite for correct chromosome segregation. In meiosis II, it is generally accepted that gametes utilize the same principle to segregate sister chromatids. Thus, the maintenance of centromeric cohesion before anaphase onset is a key for faithful segregation of chromosomes in mitosis and meiosis.

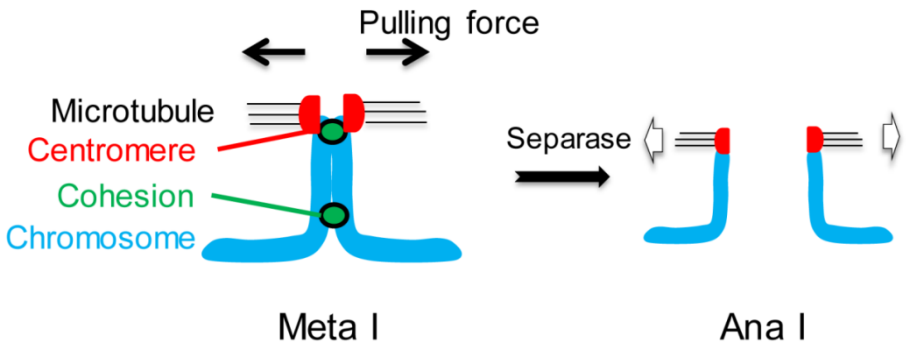

Fig. 1: Centromeric cohesion is necessary for correct chromosome segregation in mitosis.

In eukaryotes, the cohesin complex holds the sister chromatids together after DNA replication, acting as the mediator of chromosome cohesion. The cohesin complex is a multi-subunit protein complex, mainly consists of three core subunits: SMC1, SMC3, and an alpha-kleisin (Fig. 2). Two SMC (structural maintenance of chromosomes protein) proteins form a crimple structure that can accept the DNA helix, and the alpha-kleisin further close the crimple, forming a tripartite ring structure that co-entraps the sister DNA strands (Haarhuis et al, 2014). The cohesin complex in meiosis is distinct from the counterpart in mitosis. In mammals, Smc1 and Scc1 (Rad21) are replaced by

Smc1β and Rec8 in meiosis, respectively (Watanabe & Nurse, 1999; Revenkova et al, 2004; Klein et al, 1999).

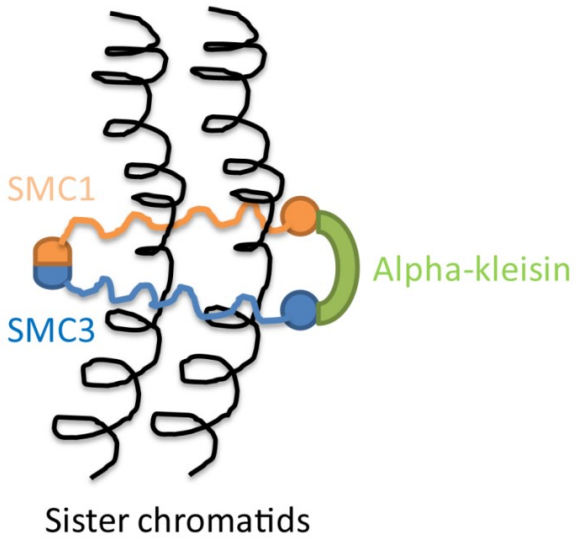

Fig. 2: Cohesin complex entraps sister chromatids.

Removal of the cohesin complex requires precise spatiotemporal regulation in cell division. There are two major waves of cohesion disassociation, which are the Wapl-dependent prophase pathway and the separase-dependent anaphase pathway. In mitosis, the Wapl pathway dissolves most but not all the cohesin complex along chromosome arms. As a result, the chromosome arms still remain partially connected, forming the discernable X-shaped chromosomes in human cells (Gandhi et al, 2006). During the metaphase-anaphase transition, after all sister chromatids are bi-oriented and the spindle assembly checkpoint (SAC) is satisfied, the anaphase-promoting complex/cyclosome (APC/C) is activated and starts to degrade inhibitors that prevent anaphase onset (Huang & Moazed, 2006). Separase, a cysteine protease, is activated after degradation of the separase inhibitor securin, and cleaves the residual

alpha-kleisin both at centromeric regions and along chromosome arms. Accompanied with the cleavage of all cohesin complex, sister chromatids are separated into two daughter cells (Hauf, 2001).

In contrast to mitosis where centromeric cohesins are removed at anaphase, in meiosis, centromeric cohesins are maintained even in the presence of separase activity at anaphase of meiosis I (anaphase I). This maintenance of centromeric cohesin ensures the persistence of cohesion between sister chromatids until metaphase of meiosis II (metaphase II), which allows bi-orientation of sister chromatids and thus correct chromatid segregation at anaphase of meiosis II (anaphase II) (Fig. 3). Thus, centromeric cohesins play a central role in the determination of chromosome segregation pattern in meiosis.

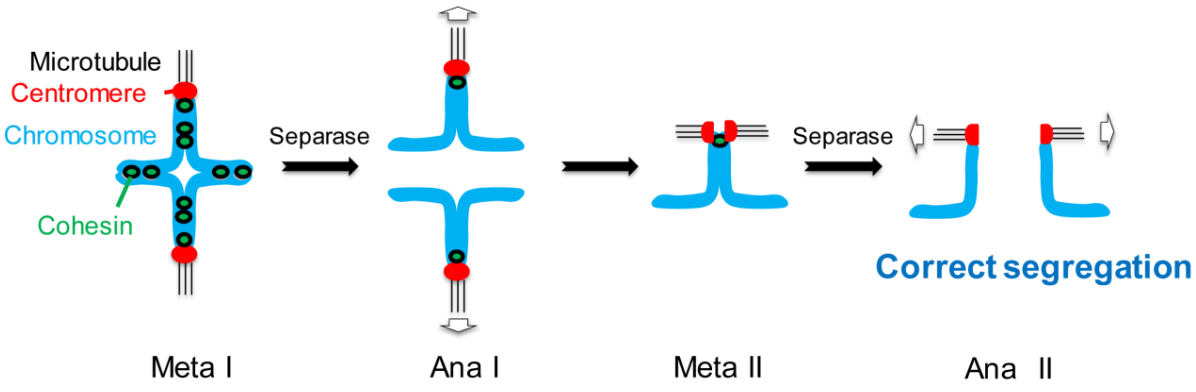

Fig 3: Centromeric cohesin is important to determine chromosome segregation manner in meiosis

Shugoshin was identified as a central player in centromeric cohesion protection. Sgo1 was found to block the degradation of Rec8, the meiosis-specific kleisin subunit of

cohesin, at centromeres at anaphase I in fission yeast (Kitajima et al, 2004). Shugoshin is a conserved protector of Rec8 in many organisms. Even before Sgo1 was identified in fission yeast, a centromere protein MEI-S332 in *Drosophila* had been characterized as a cohesion protector. Mutations in MEI-S332 lead to premature sister chromatid separation in meiosis (Kerrebrock et al, 1995). In mammals, the Sgo1-PP2A complex protects cohesin from premature removal by mitotic kinases and Wapl at centromeres in prophase pathway during mitosis (Liu et al, 2012). On the other hand, in meiosis, Sgo2 is important for centromeric cohesin protection while Sgo1 is dispensable. Both shugoshin proteins recruit PP2A-B56 to dephosphorylate alpha-kleisin in mammals, which makes them resistant to separase activity (Ishiguro et al, 2010; Katis et al, 2010). However, both Sgo1 and Sgo2 are delocalized from centromeres after anaphase I in fission yeast and mice (Kitajima et al, 2004; Lee et al, 2008). In mitosis, this delocalization presumably helps the resolution of sister chromatids. However, in meiosis, centromeric cohesin needs to be maintained until the end of metaphase II. How centromeric cohesin is protected after anaphase I is still an open question.

There are constitutive centromeric components capable of recruiting meiosis-specific factors to centromeres during meiosis. In fission yeast, Moa1 interacts with Rec8 and establishes the mono-orientation of kinetochores. Proper localization of Moa1 requires Cnp3, the homologue of CENP-C (Yokobayashi & Watanabe, 2005). In budding yeast, the monopolin complex regulates different types of kinetochore-microtubule attachment, ensuring sister chromatid co-orientation. Moreover, the monopolin subunit Csm1 physically binds Mif2/CENP-C (Corbett et al, 2010). MEIKIN was identified as a functional orthologue of Moa1 in mice, which is also presumably targeted to

centromeres by CENP-C (Kim et al, 2015). In summary, these mono-orientation-defining factors share a conserved pathway in yeast and mice. Thus, it is plausible that the constitutive centromere component CENP-C acts as a scaffold, recruiting other components responsible for meiosis-specific functions (Tanaka et al, 2009).

SUMO proteins are a family of small ubiquitin-like proteins, which covalently bind to substrate proteins. Similar to the ubiquitination process, SUMO is first activated by the cysteine-specific SUMO proteases through cleavage of extra amino acids of the C-terminus. The exposed di-glycine motif is subsequently linked to the E1 ligase, a dimer consisting of Sae1 and Sae2. Through thioester linkage, SUMO is transferred to the E2 ligase. At last, the E3 ligases pass SUMO to their target subtracts (Fig. 4). Unlike ubiquitination, sumoylation of protein does not necessarily result in the degradation of target proteins.

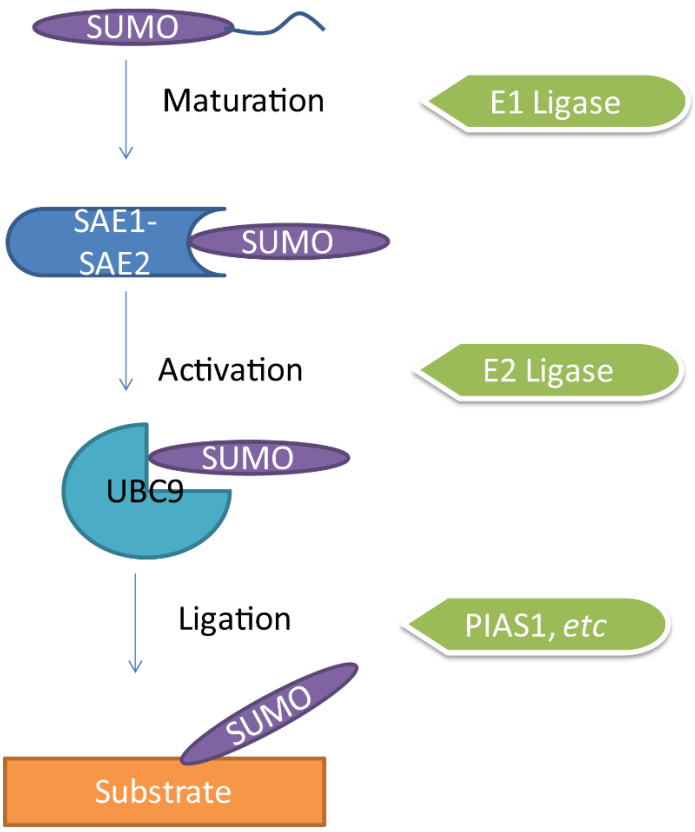

Fig 4: Sumoylation is a 3-step post-translational modification process.

Growing evidence shows that sumoylation also plays an important function in chromosome segregation. The sumoylation of centromere components regulates the localization of CENP-E at kinetochores. When sumoylation is inhibited by overexpression of the SUMO isopeptidase SENP2, CENP-E failed to localize at centromeres and chromosome congression was impaired (Zhang et al, 2008). In *C. elegans*, AIR-2 is shown to be modified by SUMO, which is stimulated by the PIAS-family protein GEI-17 in a dosage-dependent manner *in vitro*. Furthermore, loss of GEI-17 affects recruitment of kinesin KLP-19 to centromeres in *C. elegans* (Pelisch et al, 2014; Pelisch et al, 2017). It is also shown that SUMO regulates the cohesin regulator Pds5 during prophase at mitosis (D'Ambrosio & Lavoie, 2014). It has been reported that

in mouse oocytes, SUMO proteins are enriched at centromeres during meiosis (Feitosa et al, 2018; Wang et al, 2010). However, the role of SUMO at centromeres during meiosis in mammalian oocytes remains unclear.

2. Materials and Methods

2.1 Molecular cloning

In this study, *E.coli* strain DH5*α* was used to construct all the plasmids and recover the plasmids from yeast. LB medium (1% Bacto TRYPTONE, 0.5% Yeast extract, 0.5% NaCl) was used for *E.coli* culture. 50 μg/ml ampicillin or 40 μg/ml kanamycin was added to select corresponding constructs. 20 g/L agar was used to solidify the medium if needed.

Target gene fragments were amplified by PrimeSTAR HS DNA polymerase (TAKARA BIO INC) according to manufacturer's recommendation. Primers were synthesized by Hokkaido System Science or FASMAC Co. PCR products or plasmids were cut and re-ligated by the standard protocol (Sambrook et al. 1989). pGEMHE plasmid series were used for all the mRNA production. For yeast two-hybrid screening, pGBK-AD and pGAD-AD were used. pGBK-AD was replaced by pBridge in yeast three-hybrid assays.

Point mutations were introduced into cDNAs by PCR-based mutagenesis and confirmed by Sanger sequencing. The mutations used in this thesis were as follows: SUMO1gg (H98Stop), SUMO2gg (V94Stop), SUMO3gg (S93Stop), SUMO3ga (G92A and S93Stop), PIAS1(dn) (C350S) (Liang et al. 2004; Yurchenko et al. 2006), and Rec8f(nc) (R262A, R434A, and R454A) (Kudo et al. 2009).

2.2 Yeast two-hybrid screening

2.2.1 Preparation of yeast culture medium

YPDA medium (1% Bacto yeast extract, 2% Bacto peptone, adenine hemisulfate 80 mg/L, 20 g/L agar was used in plate) was used to plate the Y2H Gold yeast strain from -80°C stock. During the screening, two types of SD medium were used.

Selective SD medium:

Components	g/100mL
SD base (Clontech)	0.67
D-Glucose	2
Agar	2

Selective medium was sterilized by autoclaving. 40mL medium was used for each plate.

Non-selective SD medium:

Components	g/100mL
SD base (Clontech)	0.67
D-Glucose	2

Agar	2
Dropout supplement (Clontech)	0.06
5N NaOH	40μL
Histidine	0.002
Adenine	0.002

Non-selective medium was sterilized by autoclaving. However, histidine and adenine were added after cooled down around 60°C to avoid degradation.

2.2.2 Preparation of cDNA library

Approximate 500 germinal vesicle stage (GV-stage) oocytes were used to extract RNA. FastTrack MAG mRNA isolation kit (Invitrogen) was used to isolate total mRNA. SMART cDNA library construction kit (Clontech) was used for reverse transcription and cDNA library construction. pGAD-BD (Clontech) plasmid was used to construct and amplify the cDNA library.

2.2.3 Transformation of yeast

Li-acetate/single strand carrier DNA/PEG method (Gietz, Schiestl 2007) was used to transform yeast with minor modifications. A single colony of Y2H Gold strain was grown overnight in 2 mL YPDA medium. Yeasts were centrifuged and washed once in 0.1M Li-acetate in TE (10 mM Tris-HCl, 1 mM EDTA, pH 7.5) buffer. 50 μL 0.1 M Li-acetate in

TE, 2μL carrier DNA (10 μg/μL), plasmid DNA (about 1 μg) were added. The mixtures were seated for 10 min and then 300 μL 50% PEG 4000 in 0.1M Li-acetate in TE was added. The mixtures were then inverted up and down for 30 min. 40 μL DMSO was then added, the mixtures were incubated at 42°C for 15 min. The cells were washed again after heat shock, and then suspended in 1mL YPDA medium and incubated for 1 hr at 30°C. At last, the yeast cells were pelleted by centrifugation resuspended in water and spread in selective SD plate.

2.2.4 Screening process

Matchmaker Gold Yeast Two-Hybrid System (Clontech) was used to carry out the yeast two-hybrid screening. Full-length CENP-C was cloned into pGBK-AD as a bait to screen the cDNA library. Colonies of cells carrying positive candidate clones were grown in selective medium. All positive clones were confirmed by plasmid extraction, retransformation and sequencing.

2.3 mRNA synthesis

pGEMHE plasmid was used for the synthesis of mRNA. Template plasmids carrying target fragments were linearized by AscI restriction endonuclease in 37°C for 2 hr or overnight. Then the linearized DNA was purified by phenol/chloroform extraction. Linearized template DNA was precipitated by ethanol and eluted in RNase-free water.

To produce mRNA used for microinjection, mMESSAGE mMACHINE T7 Transcription Kit (Ambion, AM1344) was used for mRNA transcription. The reaction was carried out according to manufacturer's instructions. The mRNA products were purified by

phenol/chloroform extraction and isopropanol precipitation. Product mRNA were resuspended in RNase-free water and stored at -80°C for further use.

2.4 Culture of oocytes

2.4.1 Handling of mice

Mouse colonies were maintained in specific pathogen-free (SPF) conditions with 12-12 hr light-dark cycle. Eight-week old B6D2F1 (the first generation of female C57BL/6 crossed with male DBA/2), inbred strain C57BL/6 and *Sgo2* knockout (C57BL/6 background) (Llano et al. 2008) female mice were used to produce oocytes or eggs.

2.4.2 Preparation of culture medium

In general, M2 medium was used for oocyte culture.

Components	g/L
Calcium Chloride·$2H_2O$	0.25137
Magnesium Sulfate (anhydrous)	0.1649
Potassium Chloride	0.35635
Potassium Phosphate, Monobasic	0.162
Sodium Bicarbonate	0.35

Sodium Chloride	5.53193
Albumin, Bovine Fraction V	4.0
D-Glucose	1.0
HEPES· Na	5.42726
Phenol Red· Na	0.0106
Pyruvic Acid· Na	0.0363
DL-Lactic Acid· Na	2.95

Medium was supplemented with 0.06 g/L potassium penicillin-G and 0.05 g/L streptomycin sulfate. The pH of the medium was adjusted to 7.2-7.4 with 1 N NaOH, and then filtered through a Millipore 0.22 μm filter with positive pressure to reduce foaming. The medium were stored at 4°C for up to 2 weeks.

For zygote culture, CZB medium was used.

Components	g/L
Sodium Chloride	4.76
Potassium Chloride	0.36
Magnesium Sulfate·7 H_2O	0.29

Potassium phosphate monobasic	0.16
Sodium Bicarbonate	2.11
D-Glucose	1
Pyruvic Acid· Na	0.03
Calcium Chloride·$2H_2O$	0.25
GlutaMAX (Gibco)	0.15
Sodium lactate (Gibco)	5.3mL
EDTA ·2Na	0.04
Albumin, Bovine Fraction V	5.0

The pH of the medium was adjusted to 7.2-7.4 with 1 N NaOH and filtered through a Millipore 0.22 μm filter with positive pressure to reduce foaming. The medium were stored at 4°C for up to 2 weeks. CZB medium was gassed with 5% CO_2 in air at 37°C for at least 2 hr prior use.

2.4.3 Inhibitors used in this study

IBMX (3-isobutyl-1-methylxanthine) was used to arrest oocytes at GV-stage. 2-D08 (Calbiochem, 505156) was tested as a potential E2 sumoylation inhibitor.

2.4.4 Handling of oocytes

Eight-week-old female mice were injected with 5 IU of PMSG (ASKA Pharmaceutical). Ovaries were removed from the mice 44-50 hr after the injection. Cumulus-oocyte complexes were released from the ovaries by mechanical shearing with 22 gauge needles and transferred into M2 medium supplemented with 200 nM IBMX at 37°C. The cumulus cells were removed from the oocytes by repeat pipetting with a mouth-controlled glass micropipette. To induce meiotic maturation, oocytes were washed with series of pre-warmed M2 medium without IBMX for 6 times and transferred to fresh medium.

Usually, healthy oocytes undergo GVBD in 1 hr after being released to fresh M2 medium. To obtain maximum number of oocytes for immunostaining, oocytes failed to undergo GVBD in 1.5 hr were discarded. However, GVBD time was defined 1 hr after being released from IBMX arresting.

To obtain oocytes at telophase I, I monitored individual oocyte for the onset of first polar body extrusion under a stereomicroscope. According to the live imaging data, onset of first polar body extrusion occurs about 6 min after anaphase I onset. I collected and fixed the oocytes approximately 1 hr after onset of the polar body extrusion. After immunostaining, oocytes with aggregated chromosomes were selected for further analysis.

To obtain *in vivo* maturated MII eggs, I injected eight-week-old BDF1 female mice with 5 IU of PMSG, and then 5 IU HCG (Human chorionic gonadotropin) after 48 hr. MII eggs

were collected from oviduct about 12 hr later. Cumulus cells were removed from the eggs by treatment with Hyaluronidase solution (80 IU/mL). Denuded eggs are washed 6 times by pre-warmed M2 and cultured in M2 medium at 37°C.

To obtain 1-cell stage zygotes, I injected eight-week-old BDF1 female mice with 5 IU of PMSG, and then 5 IU HCG and crossed the females with BDF1 male mice after 48 hr. Female mice were sacrificed 18 hr after HCG injection. 1-cell stage zygotes were collected by flushing oviduct. Then zygotes were washed 6 times by pre-warmed M2 and cultured in CZB medium gassed with 5% CO_2 in air at 37°C.

2.5 Microinjection of RNAs or antibody

The synthesized RNAs or antibody were introduced into mouse oocytes or egg through microinjection. Microinjection was implemented with Narishige micromanipulator equipped with piezo impact drive system (Prime Tech). To maintain 37°C during manipulation, a Tokai Hit Thermoplate system was used to heat up the oil dish. Injection volume was controlled with an ocular micrometer. The injection volume was calibrated by measuring the diameter (d) of an oil drop. The volume of injected solution was calculated by the following equation:

$$V=4/3 \cdot \pi \cdot (d/2)^3$$

The injection volume corresponds less than 5% of the oocyte volume. The microinjected GV-oocytes were incubated for 2-3 hr in M2 medium supplemented with 200 nM IBMX at 37°C before induction of meiotic resumption.

For egg microinjection, *in vivo* maturated MII eggs were used. As MII egg membrane is much more elastic than GV-stage oocytes, microinjection was carried out at ambient temperature without heat plate.

Amount of mRNAs used in microinjection: 0.5 pg H2B-mCherry, 0.5 pg mEGFP-PIAS1, 0.5 pg mEGFP-PIAS2, 0.5 pg mEGFP-PIAS3, 0.5 pg mEGFP-PIAS4, 1 pg mNG-SUMO1, 1 pg mNG-SUMO3, 1 pg mNG-SUMO1gg, 1 pg mNG-SUMO2gg, 1 pg mNG-SUMO3gg, 1 pg mNG-SUMO3ga, 0.5 pg of mEGFP-PIAS1(dn), 0.5 pg mNG-PIAS1(dn), 1.5 pg PIAS1(dn)-CENP-C, 1.5 pg PIAS1-CENP-C,1.5 pg CENP-C, 1 pg mNG-CENP-C, 1 pg mNG-PIAS1(dn), 1 pg mNG-PIAS1(dn)-CENP-C, 1 pg mNG-PIAS1(dn)-Rec8f-CENP-C, 1 pg mNG-PIAS1(dn)-Rec8f(nc)-CENP-C, 1pg PIAS1(dn)-Rec8f-CENP-C, 1 pg PIAS1(dn)-Rec8f(nc)-CENP-C, 1.5 pg mEGFP-Rec8f-mCherry-CENP-C, 4 pg PP2A-B56ε-mNG, 0.5 pg Sgo2-24xGCN4 , 0.5 pg scFv-sfGFP.

2.6 Live imaging

4-well LabTek chambered coverglass (Nunc) was used for live imaging. Oocytes were cultured in fresh M2 medium drops covered with mineral oil. In case of inhibitor was added in the culture, 8-well LabTek was used. 200-300μL M2 supplemented with the inhibitor was used for each well. The chambers were sealed by silicone grease (Bayer, 85403). Time-lapse imaging was performed with a Zeiss LSM780 microscope automated by a 3D multi-location tracking macro (Rabut, Ellenberg 2004). A 40xC-Apochromat 1.2NA water immersion objective lens was used. Eleven confocal z sections (2.5-μm interval) of 400 × 400 pixel xy images covering 30.36 × 30.36 × 27.5

μm were recorded at 8 or 10-min time intervals. For kinetochore tracking analysis at late metaphase I, a z stack containing 21 z-slices (1.2 μm) of 512 × 512 pixel xy image covering 30.23 × 30.23 × 25.2 μm was captured at 2-min intervals. To minimize the damage due to laser illumination, oocytes were imaged 6 hr after being released from GV-stage.

2.7 Immunofluorescence staining

Oocytes were fixed with 1.6% PFA in 10 mM PIPES pH 7.0, 1 mM $MgCl_2$ and 0.1% Triton X-100 for 30 min. After fixation, the oocytes were washed 6 times by PBT (PBS supplemented with 0.1% Triton X-100). The oocytes were preserved and permeabilized with PBT at 4°C overnight. The oocytes were blocked with 3% BSA-PBT for 1 hr at room temperature or overnight at 4°C. First antibodies were diluted in 3% BSA-PBT. After overnight incubation with first antibodies at 4°C, the oocytes were washed with 3% BSA-PBT 4 times, and then incubated with secondary antibodies for 2 hr at ambient temperature or overnight at 4°C. The oocytes were washed twice with 3% BSA-PBT, twice with PBT, twice with 0.01% BSA-PBS and stored in 0.01% BSA-PBS (supplemented with Hoechst33342 at a final concentration of 5 μg/mL). The prepared samples were imaged immediately or stored at 4°C for later imaging.

For PIAS1 staining, a pre-extraction protocol was adopted. After harvesting oocytes, I treated the oocytes with Tyrode's solution (Irvine Scientific) briefly to remove zona, and then washed the zona-free oocytes with pre-warmed M2 medium supplemented with IBMX. Zona-free oocytes were recovered at 37°C for at least 30 min. After recovering, oocytes were washed with pre-warmed M2 medium for 6 times, and then cultured in M2

medium to allow maturation. Oocytes failed to undergo GVBD in 1.5 hr were discarded. Zona-free oocytes were pre-extracted with 0.25% Triton X-100 in 60 mM PIPES, 25 mM HEPES pH 7.0, 10 mM EGTA, 4 mM $MgSO_4$ for 5 sec before fixation.

For Rec8 staining, a microinjection method was performed. Rec8 antibody was buffer exchanged by centrifugal filters (10k, Amicon Ultra). Antibody was concentrated with PBS buffer. The final concentration of antibody was determined by Bradford method (BioRad). Series of BSA were used as standards to calibrate the curve. 4 pg of anti-Rec8 antibody was microinjected into living oocytes at metaphase II stage, and then oocytes were fixed after 8 min incubation in 37°C. The following steps were the same as immunostaining protocol used in this study.

First antibodies used in immunofluorescence: Human anti-centromere antibodies (ACA, Antibodies Incorporated, 1:100), Mouse anti-SUMO2/3 (MEDIMABS, 1:200), Mouse anti-SUMO1 (MBL, 1:200), Rabbit anti-pericentrin (Abcam, 1:500), Rabbit anti-PIAS1 (Cell Signaling, 1:200), Mouse anti-Sgo2 (gift from Dr. Watanabe, 1:200), Rabbit anti-Sgo2 (gift from Dr. Watanabe, 1:300), Rabbit anti-Smc3 (Abcam, 1:200), Rabbit anti-Rec8 (MBL).

Secondary antibodies used: Alexa Fluor 488 goat anti-mouse IgG (H+L) Alexa Fluor 488 goat anti-rabbit IgG (H+L) Alexa Fluor 488 goat anti-human IgG (H+L) Alexa Fluor 555 goat anti-mouse IgG (H+L) Alexa Fluor 555 goat anti-human IgG (H+L) Alexa Fluor 555 donkey anti-sheep IgG (H+L) Alexa Fluor 647 goat anti-human IgG (H+L), all of them were purchased from Molecular Probes (Life technologies). The secondary antibodies were used at 1:500 dilutions.

Imaging acquisition was carried out in a 4-well LabTek chambered coverglass (Nunc). A Zeiss LSM780 microscope with GaAsP detector was used to imaging the samples. A 40xC-Apochromat 1.2NA water immersion objective lens was used to capture the images. Typically, 512 × 512 pixel xy image covering 30.23 × 30.23 μm was captured at 1 μm step in z axis, for Rec8 imaging, a 0.25 μm z step was used.

2.8 Quantification of immunostaining and live imaging

2.8.1 Fluorescence signal quantification

To determine the relative level of PIAS1 around centromeres, I measured the mean signal intensity of PIAS1 around the peak of the signal and subtracted by the signal intensity of cytoplasmic region near the peak signal. The level of the ACA signal of the same centromere was measured by the same way. The ratio between the levels of PIAS1 and ACA was calculated to determine the relative level of PIAS1. Over 5 centromeric signals were analyzed and averaged for each oocyte. Relative levels of SUMO2/3, SMC3, Rec8, and Sgo2 signals to the ACA signals were quantified by the same method.

To quantify the levels of fluorescent tagged protein in live imaging, I measured mean signal intensity around the peak of the signal and then subtracted by the average cytoplasm signal intensity. To quantify the levels of PP2A-B56ε-mNeonGreen (mNG), the mean signal intensity was measured around the peak of the signal and then subtracted by the average signal intensity on the chromosome. More than 5 centromeric

signals were quantified for each oocyte at each time point. Signal intensities near chromosomes were measured when no centromeric enrichment was observed.

2.8.2 Kinetochore tracking

Kinetochore tracking was performed as previously described (Kitajima et al. 2011; Sakakibara et al. 2015). Kinetochore signals were peak-enhanced and background-subtracted with a combination of Gaussian filters in Fiji (Schindelin et al. 2012). The image series around anaphase I onset were then reconstructed into 3D stacks in Imaris software (Bitplane). All kinetochore positions were determined and tracked manually. Sister kinetochore pairs were manually determined based on alignment and distance. Positions of the kinetochores, inter kinetochore distances are extracted from Imaris. The kinetochore positions and tracks were visualized with Pov-Ray software (http://www.pov-ray.org) from data generated by an in-house Java program.

2.8.3 3D reconstruction of sister kinetochore positons

3D reconstruction of the kinetochore positions were carried out in Imaris software (Bitplane) based on the high resolution immunostaining images. To assist the designation of sister kinetochore pairs, the cosine values of the angles between sister kinetochore axis and spindle axis were also calculated. Sister kinetochore pairs were designated by the nearest inter-kinetochore distance and minimum angles of paired kinetochore axis. The kinetochore positions were extracted from Imaris and visualized with Pov-Ray software (http://www.pov-ray.org) from data generated by an in-house

Java program. Normal sister pairs were defined by two criteria: inter-kinetochore distance was smaller than 3.0 μm, the cosine value of the angle for the sister kinetochore axis is greater than 0.8. Precociously separated sister chromatid was defined if the inter-kinetochore distance was larger than 3.0 μm. Misaligned chromosome with weak cohesion was defined with an inter-kinetochore distance between 2.2-3.0 μm and a cosine value smaller than 0.8. The left kinetochore pairs were defined as misaligned chromosomes.

2.9 Statistical analysis

Prism 6 software (GraphPad) was used for statistical analysis. Student's t-test was used to test the significance if not specified.

3. Results

3.1 Sgo2 is delocalized from kinetochores after anaphase I onset

To achieve correct chromosome segregation, centromeric cohesion must be maintained through the transition of meiosis I and meiosis II. The conserved protein shugoshin is known to act as a protector for the maintenance of the centromeric cohesion at anaphase I onset. However, whether shugoshin can protect centromeric cohesion during late anaphase I and telophase I remains unclear. In fission yeast, shugoshin Sgo1 is detectable at centromeres at the onset of anaphase I but undetectable at late anaphase I. Similarly, in mammals, the functional orthologue Sgo2 is not detected at late anaphase I. To quantitatively describe the kinetics of Sgo2 delocalization after anaphase I onset in mouse oocytes, I aimed to conduct high resolution live imaging of Sgo2. To achieve this, I used the SunTag system, which

amplifies the fluorescent signals in living cells and thus allows us to minimize the expression levels of exogenously introduced tagged proteins. I microinjected the *in vitro*-synthesized mRNA of the Sgo2-SunTag construct together with H2B-mCherry into oocytes at the germinal vesicle (GV) stage. I then monitored the dynamics of Sgo2-SunTag from metaphase I to metaphase II.

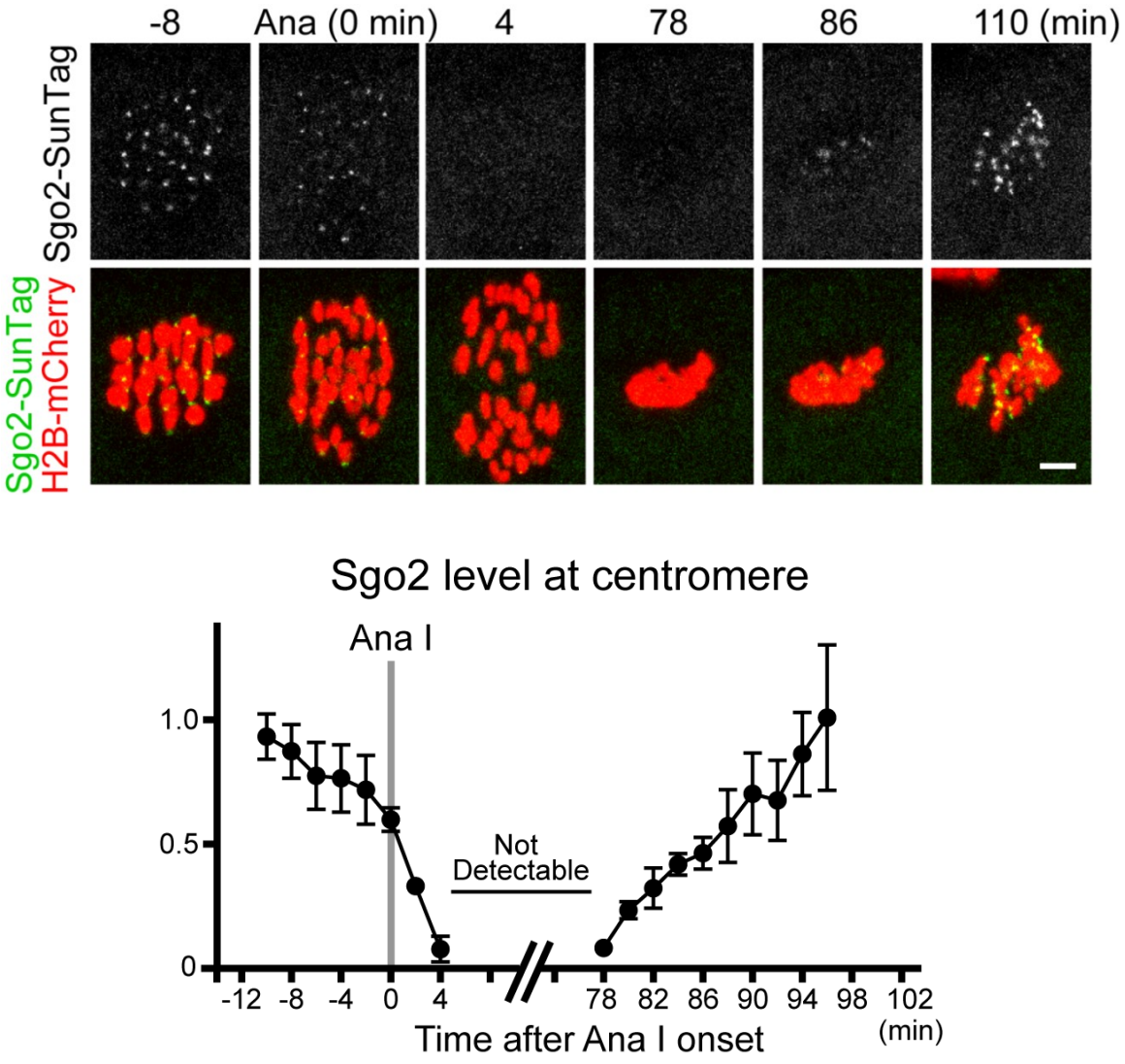

Fig. 5: Sgo2 is delocalized from centromeres after anaphase I. Time-lapse imaging of oocytes expressing Sgo2-SunTag (green) and H2B-mCherry (red). Scale bar is 5 μm.

Sgo2-SunTag intensity was quantified and plotted (n=4 oocytes). Time after anaphase I onset (min). Error bars show the SD. (Ding *et al*, *Curr. Biol.* 2018)

Sgo2-SunTag showed clear kinetochore signals during prometaphase I, metaphase I and prometaphase II, consistent with the Sgo2 localization data in previous report (Lee et al. 2008). After anaphase I onset, Sgo2-SunTag signals underwent a sharp decrease. I quantified the Sgo2-SunTag intensity at centromeres around anaphase I. Sgo2-SunTag signals already showed a steady decrease even before anaphase I onset. Afterwards, it showed the highest decreasing rate from 0 to 4 min after anaphase I onset. Sgo2-SunTag signals then became undetectable in 5 min after anaphase I onset. Afterward, Sgo2-SunTag still stayed at undetectable levels until prometaphase II, when the chromosomes started to individualize again (Fig. 5). These results suggested that in mouse oocytes Sgo2 is sharply delocalized from centromeres after anaphase I onset and stay undetectable at anaphase I until prometaphase II.

3.2 PP2A-B56 is decreased at kinetochores after anaphase I onset

Sgo2 recruits the protein phosphatase 2A (PP2A)-B56 to centromeres, which makes cohesin resistant to separase activity. I therefore tested whether PP2A-B56 is delocalized from centromeres together with Sgo2 after anaphase I onset. To quantitatively analyze kinetics of PP2A-B56 after anaphase I, I performed high resolution live imaging of PP2A-B56. A live imaging marker for PP2A-B56, PP2A-B56ε-mNG, has already been established in my lab (Yoshida et al. 2015). I microinjected mRNA of PP2A-B56ε-mNG together with H2B-mCherry into GV stage oocytes, and then imaged the dynamics of PP2A-B56ε-mNG localization from

metaphase I to metaphase II. Quantification showed that PP2A-B56ε-mNG signal intensity decreased steadily 10min before anaphase I onset until about 60min after anaphase I onset, and then gradually recovered during prometaphase II (Fig. 6). It is notable that the decreasing rate of PP2A-B56ε was much slower than Sgo2, which can be explained by the multiple recruitment pathway of PP2A-B56ε. Taken together, our results confirmed that both Sgo2 and PP2A-B56ε underwent a substantial decreasing after anaphase I onset, which raises a question that how cohesion is maintained at post-anaphase I.

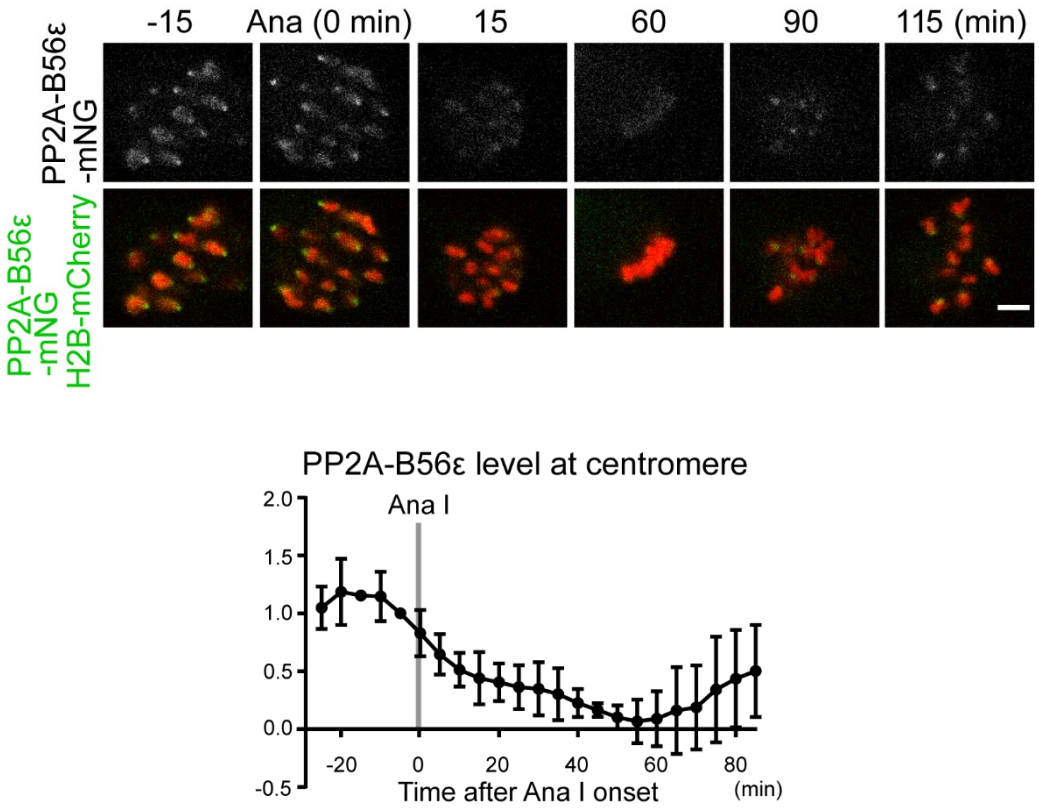

Fig. 6: PP2A-B56ε is removed from centromeres after anaphase I onset. Time-lapse imaging of oocytes expressing PP2A-B56ε-mNG (green) and H2B-mCherry (red). Scale bar is 5 μm. Signal intensity of PP2A-B56ε-mNG was quantified and plotted (n= 5

oocytes). Time after anaphase I onset (min). Error bars show the SD. (Ding *et al*, *Curr. Biol.* 2018)

3.3 PIAS1 is identified as an interactor of CENP-C by Y2H

To identify the candidate proteins responsible for protection of centromeric cohesion during post-anaphase I periods in meiosis, Dr. Masako Kaido in my lab set up a screening system by yeast two-hybrid. As CENP-C is a well-known scaffold protein responsible for meiosis-specific centromere functions, she used CENP-C as a bait to screen against the cDNA library prepared from GV-stage oocytes. This screening identified 14 positive clones as interactor with CENP-C. Out of the 14 clones, 12 individual genes were identified as interactor with CENP-C after sequencing and retransformation with full-length coding DNA sequences (CDSs) (table 1).

MGI	Gene Symbol	Description	No. of clones	EGFP fusion Localization
1913125	PIAS1	E3 SUMO-protein ligase	2	Kinetochore
104860	Fxr1	fragile Xmental retardation gene 1, autosomal homolog	2	Cytoplasm
2385758	Ablim2	actin-binding LIMprotein 2	1	Cortex
1914738	Calcoco1	calcium binding and coiled coil domain 1	1	Not tested
1351331	Chaf1	a chromatin assembly factor 1, subunit A (p150)	1	Not tested
106613	Dvl2	dishevelled 2, dsh homolog (Drosophila)	1	Cytoplasm
108100	Dvl3	dishevelled 3, dsh homolog (Drosophila)	1	Not tested
106598	Myo5b	myosin VB	1	Not tested
1917029	Pphln1	periphilin 1	1	Not tested
1921584	Ranbp10	ran-binding protein 10	1	Not tested
101838	Tbp	transcription initiation factor TFIID subunit 1	1	Not tested
2443713	Ythdc1	YTH domain containing 1	1	Cytoplasm

Table 1: List of genes obtained from two-hybrid screening of a cDNA library from GV stage oocytes with the bait CENP-C. The positive interactions in the two-hybrid assays were confirmed through retransformation. (Ding *et al*, *Curr. Biol.* 2018)

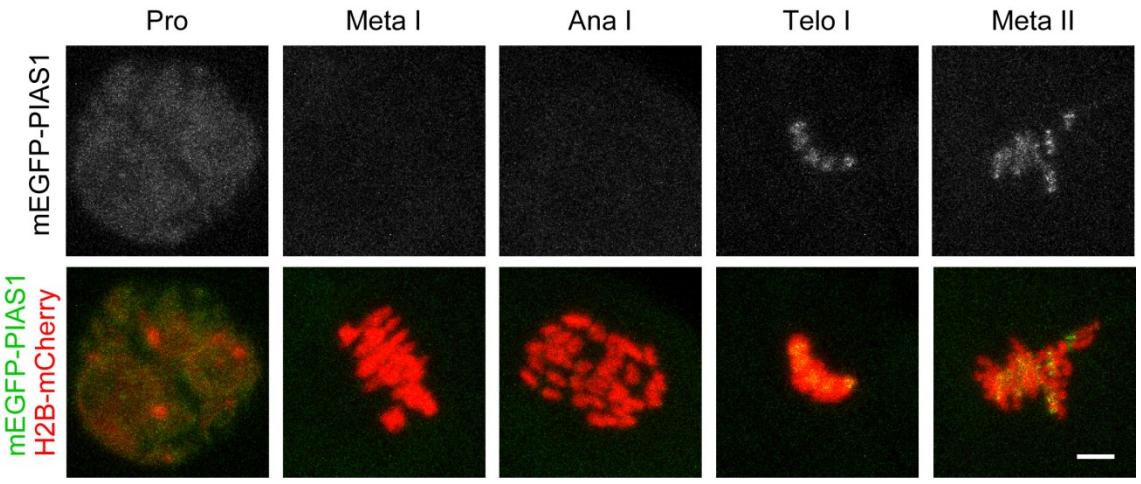

Fig. 7: PIAS1 can localize near centromeres. Oocytes expressing mEGFP-PIAS1 (green) and H2B-mCherry (red) were imaged. Scale bar is 5 μm. (Meta II, Ding *et al*, *Curr. Biol.* 2018)

To further narrow down candidate genes, I performed a secondary live imaging based screening with full-length CDSs of candidate genes fused with mEGFP gene. These mEGFP fused proteins were used as markers to further investigate their localization patterns during meiosis. I microinjected mRNA of these markers together with H2B-mCherry into GV-stage oocytes and allowed them to mature *in vitro*. I used confocal microscope to monitor the dynamics of these markers. This live imaging based secondary screening found that PIAS1, an E3 sumoylation ligase, localized near centromeres at telophase I and metaphase II (Fig. 7). These results suggested that PIAS1 is a candidate for centromeric cohesion protection during post-anaphase I stages.

After finding PIAS1 as a candidate for centromeric cohesion protection during post-anaphase I, I narrowed down the regions of CENP-C required for the interaction by

yeast two-hybrid. Yeast two-hybrid results showed that the C-terminus of CENP-C is responsible for the interaction with PIAS1 protein (Fig. 8).

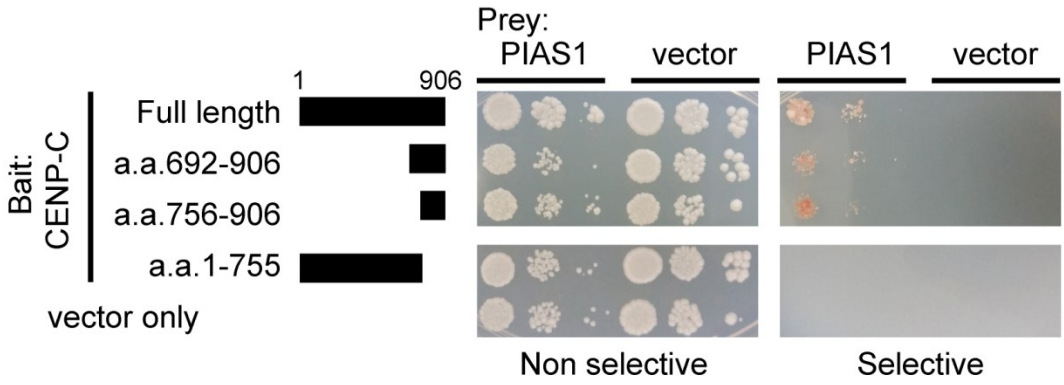

Fig. 8: PIAS1 interacts with CENP-C. Interactions were tested by yeast two-hybrid assays. (Ding *et al*, *Curr. Biol.* 2018)

Interestingly, this C-terminus region of CENP-C is also responsible for MEIKIN binding (Kim et al. 2015). Considering that both MEIKIN and PIAS1 are expressed during meiosis I, it is expected that they may compete for CENP-C binding. Then, I set up a yeast three-hybrid system to test this idea. pBridge plasmid was used to express the bait CENP-C protein, pGAD-AD plasmid was used to express the prey PIAS1 protein, then I expressed the third protein MEIKIN in the pBridge plasmid to test whether MEIKIN can compete with PIAS1 for CENP-C binding. In the yeast three-hybrid assays, interaction between CENP-C and PIAS1 was confirmed as in yeast two-hybrid (Fig. 8, 9). As expected, after the third protein MEIKIN was expressed in yeast, the interaction between CENP-C and PIAS1 was inhibited (Fig. 9), suggesting that MEIKIN can compete with PIAS1-CENP-C interaction. Intriguingly, MEIKIN appears at centromeres during the pachytene stage, persists until metaphase I, and disappears after anaphase I

(Kim et al. 2015). Meanwhile, PIAS1 starts to enrich near centromeres after anaphase I. These data suggest that MEIKIN disassociates from centromeres, which may provide free binding sites for PIAS1 after anaphase I.

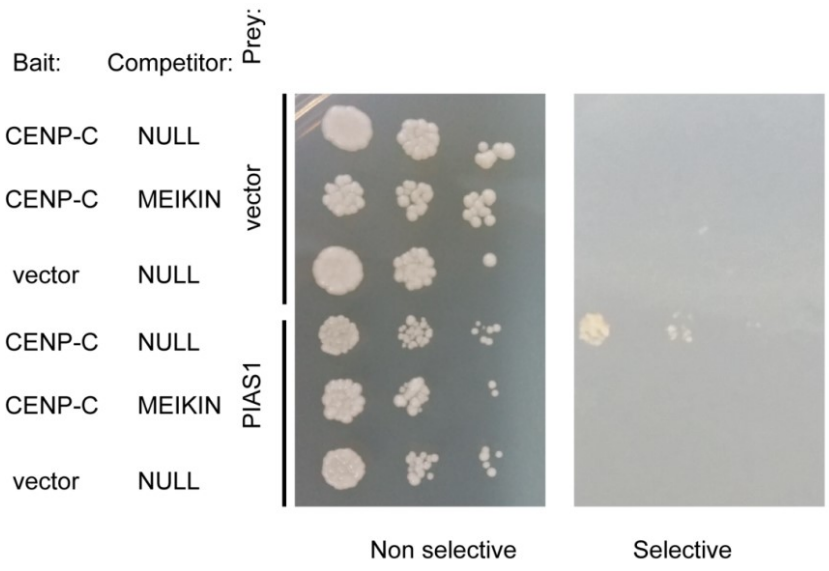

Fig. 9: MEIKIN competes with PIAS1 for CENP-C binding sites, tested by yeast three-hybrid assays.

There are 4 PIAS protein family members in the mouse genome. Sequence alignments showed that PIAS family proteins shared up to 60% amino acid sequence identity, which raised a possibility that they may act redundantly during meiosis. First, I tested whether they are expressed in meiosis or not. By PCR I managed to clone all PIAS family genes from the GV-stage cDNA library, showing that all of them are expressed during meiosis. Then I checked whether they share the same dynamics in meiosis by live imaging. I made the fused mEGFP-PIAS2-4 constructs and microinjected their mRNAs with H2B-mCherry mRNA to track their localization patterns during meiosis.

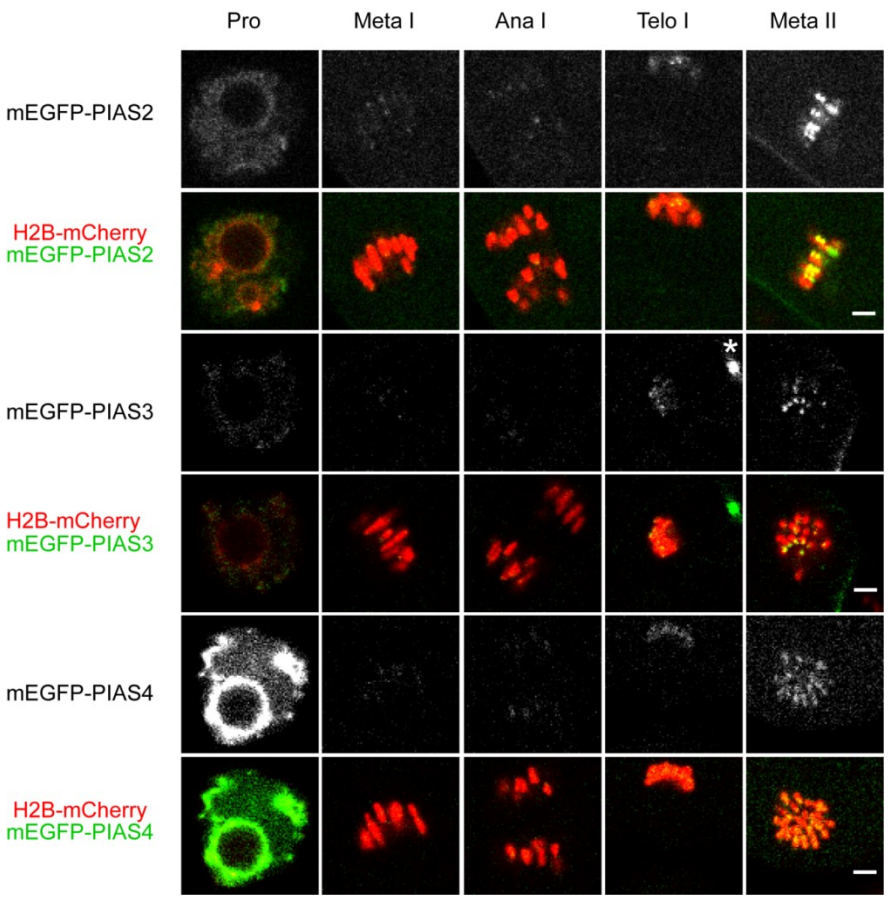

Fig. 10: All PIAS family members can localize to centromeres. mEGFP-tagged PIAS2, PIAS3 or PIAS4 (green) were expressed with H2B-mCherry (chromosomes, red) in oocytes. Asterisk indicates signals at the spindle midzone. Scale bar is 5 μm. (Meta II, Ding *et al*, *Curr. Biol.* 2018)

Live imaging data showed that all four PIAS proteins started to enrich near centromeres after anaphase I and persisted until metaphase II (Fig. 7, 10). These results suggested that all four PIAS proteins have a capacity to localize near centromeres and share similar dynamics during meiosis.

3.4 PIAS1 and SUMO2/3 are enriched at telophase I

3.4.1 PIAS1 is enriched near centromeres at telophase I

In the live imaging data, mEGFP-PIAS1 started to localize near centromeres after anaphase I onset and kept on accumulating until metaphase II (Fig. 7). However, I noticed that in mEGFP-PIAS1 overexpression conditions, some chromosomes failed to align at the spindle equator at metaphase II (Fig. 7), which suggested that the persistence of high levels of mEGFP-PIAS1 at centromeres might not reflect the physiological dynamics of PIAS1. It is possible that there were artifacts in the live imaging of mEGFP-PIAS1 under overexpression condition. Then I inspected the dynamics of endogenous PIAS1 by immunostaining. I fixed oocytes at metaphase I (4 hr after GVBD), telophase I (1.1 hr after anaphase I onset) and metaphase II (12-14 hr after GVBD) and stained for PIAS1 and centromeres (ACA). I normalized centromeric PIAS1 intensities relative to ACA intensities by a ratiometric quantification approach. Consistent with the live imaging results, endogenous PIAS1 localized near centromeres through meiosis. However, unlike the live imaging data of mEGFP-PIAS1, the endogenous PIAS1 protein level near centromeres was enriched during telophase I, and then decreased at metaphase II (Fig. 11). Considering the defects observed in mEGFP-PIAS1-overexpression oocytes at metaphase II, I concluded that PIAS1 is localized near centromeres, and this localization is enhanced at telophase I and decreased at metaphase II.

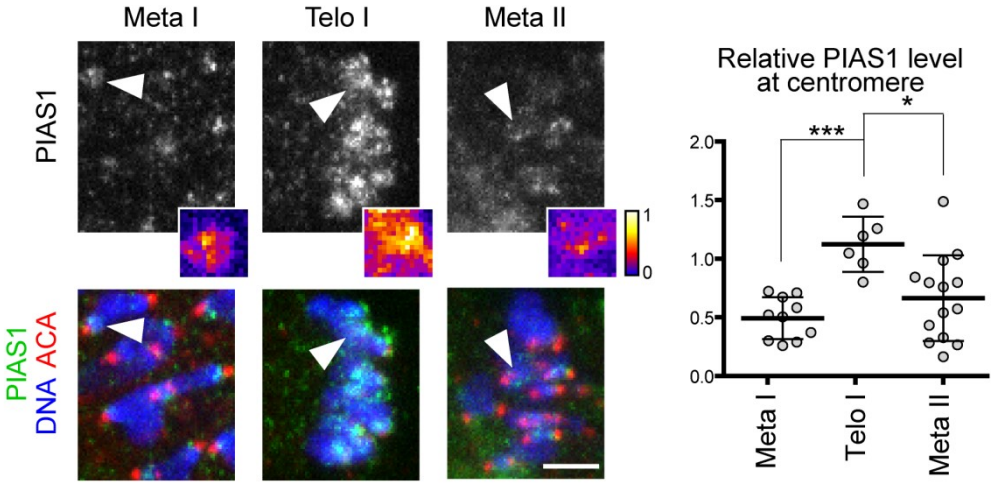

Fig. 11: Endogenous PIAS1 are enriched near kinetochores at telophase I. Oocytes at metaphase I (4 hr after GVBD), telophase I (1.1 hr after anaphase I onset), and metaphase II (12–14 hr after GVBD) were stained for PIAS1 (green), centromeres (ACA, red), and DNA (Hoechst 33342, blue). The signals indicated with arrowheads were magnified with fire color coding. The levels relative to ACA signals are shown (n = 10, 6, and 14 oocytes). Scale bar is 5, Error bars show SD. *p<0.5, ***p<0.0001. (Ding *et al*, *Curr. Biol.* 2018)

3.4.2 SUMO2/3 but not SUMO1 are enriched near centromeres at telophase I

PIAS1 is an E3 sumoylation ligase, which incorporates SUMO to substrates. I therefore expected that SUMO proteins are also enriched near centromeres at telophase I. There are three SUMO genes in the mouse genome, namely SUMO1, SUMO2, and SUMO3. SUMO2 and SUMO3 are nearly identical (97% identity) and likely have redundant functions (O'Rourke et al, 2013; Hay, 2005). At first, I evaluated the dynamics of SUMO proteins by live imaging. I made the mNG-SUMO1, -SUMO2, and –SUMO3 constructs,

microinjected their mRNAs with H2B-mCherry, and performed live imaging. However, I found that these constructs failed to produce any visible signals after GVBD, although they showed nuclear signals at GV-stage (Fig. 12).

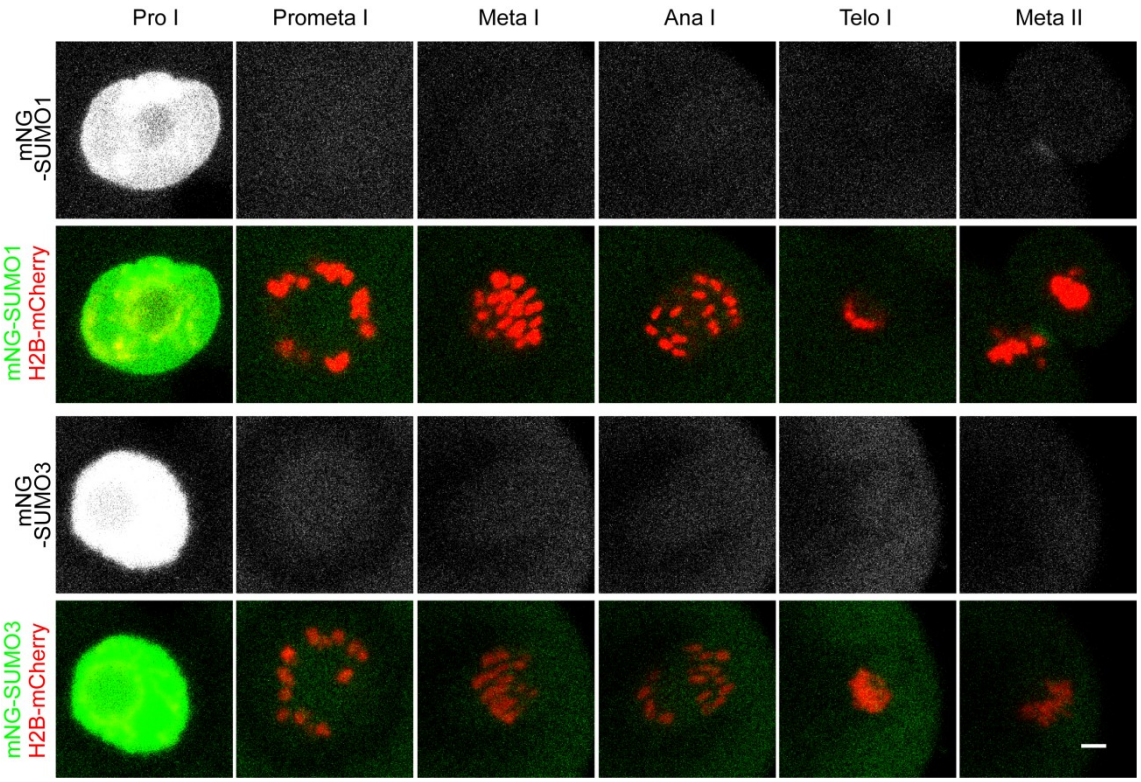

Fig.12: mNG-SUMO1 and -SUMO3 failed to localize near centromeres. Oocytes expressing mNG-SUMO1gg or -SUMO3gg (green) and H2B-mCherry (chromosomes, red) were imaged. Scale bar is 5 μm.

I reasoned that this failure may be due to a failure of exogenous mNG-SUMOs to compete with endogenous SUMOs during the sumoylation process because there is a huge pool of free SUMOs in oocytes (Huang et al, 2015). To overcome this problem, I truncated full-length SUMO genes so that their protein products ended with processed amino acids GG (glycine-glycine) at the C terminus (naming mNG-SUMO1gg,

mNG-SUMO2gg and mNG-SUMO3gg), which are known to be readily incorporated into sumoylation process (Alonso et al, 2015). Then I expressed these three constructs with H2B-mCherry and monitored their dynamics by live imaging.

Live imaging of mNG-SUMO1gg showed unknown spot-like structures around the spindle during early prometaphase I (2-3 hr after GVBD) and disappeared afterward, and there was no enriched signals near centromeres during the whole meiosis process (Fig. 13).

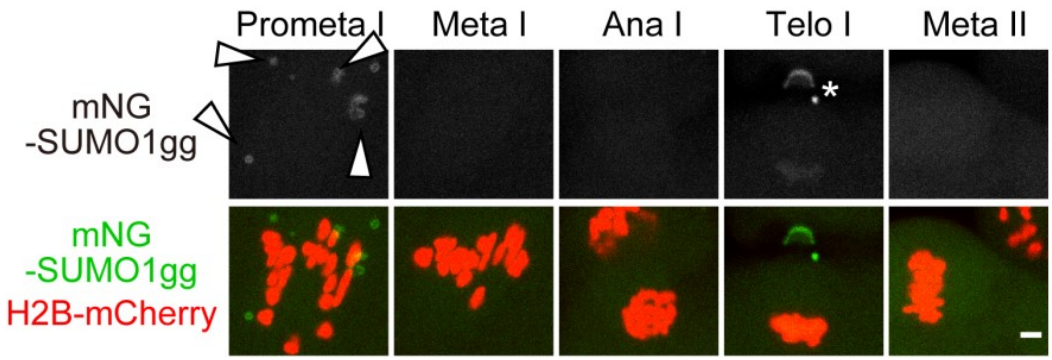

Fig. 13: SUMO1 shows no enrichment near centromeres. Oocytes expressing mNG-SUMO1gg (green) and H2B-mCherry (chromosomes, red) were imaged. Arrowheads indicate the punctuate signals of mNG-SUMO1gg. Asterisk indicates signals at the spindle midzone. Scale bar is 5 μm. (Ding *et al*, *Curr. Biol.* 2018)

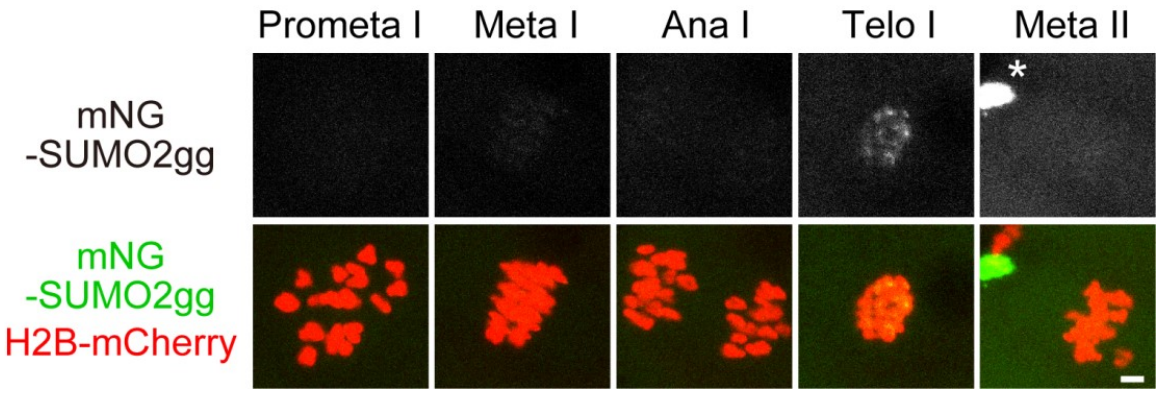

Fig. 14: mNG-SUMO2gg is enriched near centromeres at telophase I. Oocytes expressing mNG-SUMO2gg (green) and H2B-mCherry (red) were imaged. Asterisk indicates signals at the spindle midzone. Scale bar is 5 μm. (Ding *et al*, *Curr. Biol.* 2018)

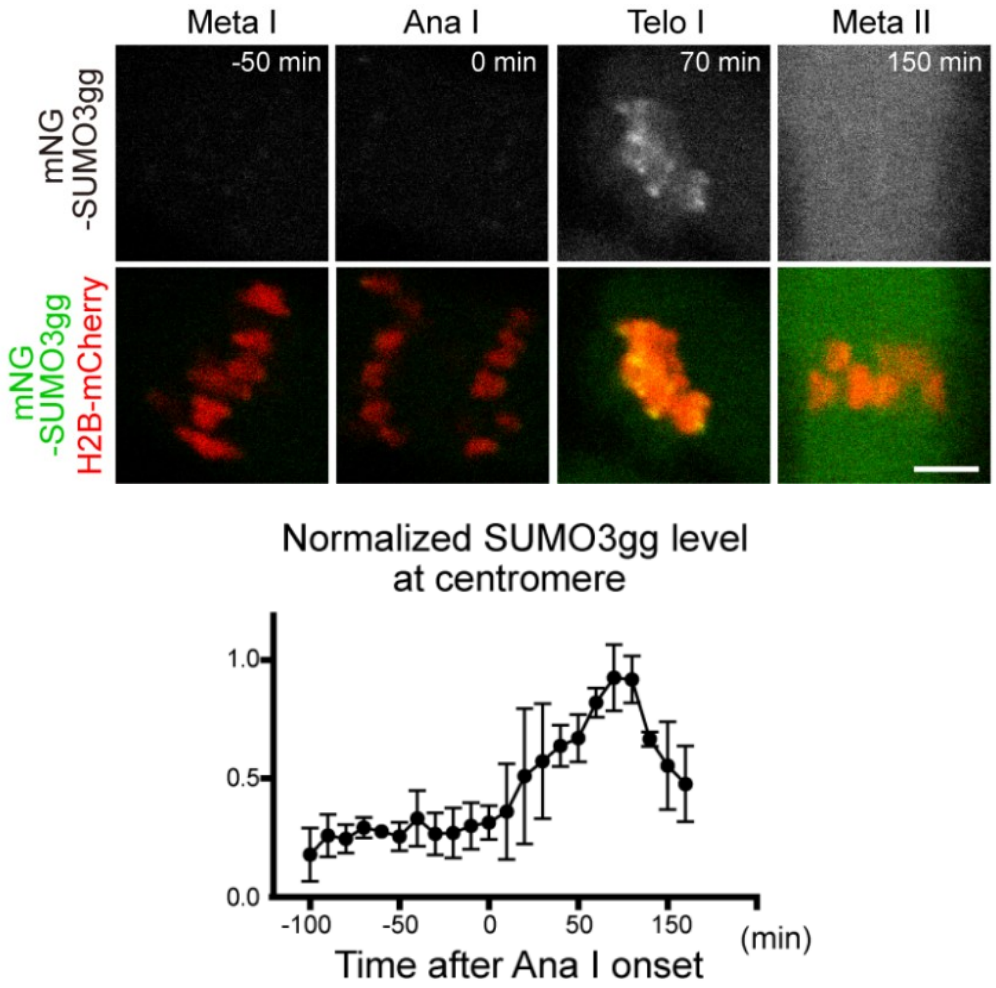

Fig. 15: mNG-SUMO3gg is enriched near centromeres at telophase I. Oocytes expressing mNG-SUMO3gg (green) and H2B-mCherry (red) were imaged and analyzed. (n=5 oocytes). Time after anaphase I onset (min). Error bars show the SD. Scale bar is 5 μm. (Ding *et al*, *Curr. Biol.* 2018)

In contrast, mNG-SUMO2gg and mNG-SUMO3gg were enriched near centromeres at telophase I (Fig. 14, 15). Quantification of mNG-SUMO3gg signals at centromeres showed that mNG-SUMO3gg was gradually enriched around centromeres after anaphase I and then steadily diminished after reaching a peak at around 80 min after anaphase I onset (Fig. 15).

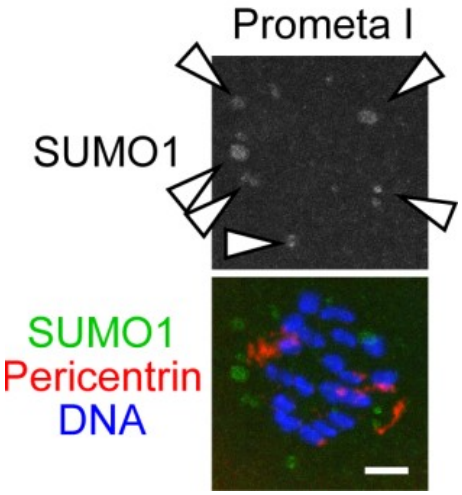

Fig. 16: SUMO1 shows no enrichment near centromeres. Oocytes at prometaphase I (2-3 hr after NEBD) were fixed and stained for SUMO1 (green), pericentrin (MTOCs, red) and chromosomes (Hoechst33342, blue). Arrowheads indicate the punctuate signals of SUMO1. Scale bar is 5 μm. (Ding *et al*, *Curr. Biol.* 2018)

To confirm the live imaging data of mNG-SUMO1gg, I fixed oocytes 2-3 hr after GVBD, and stained for SUMO1, pericentrin and chromosomes. Endogenous SUMO1 showed cytoplasmic foci at early prometaphase I (2.5 hr after GVBD), consistent with the live imaging data (Fig. 16). The triple staining result showed that SUMO1 foci did not overlap with the microtubule-organizing center (MTOC) structures. As SUMO1 was not

enriched near centromeres where PIAS proteins localize during meiosis, it is possible that sumoylation by SUMO1 is not mediated by PIAS family proteins.

To confirm mNG-SUMO2/3gg live imaging, I fixed oocytes at 4 hr after GVBD, 1.1 hr after anaphase I onset, 12-14 hr after GVBD, and stained for SUMO2/3 and centromeres (ACA). Immunostaining data showed that SUMO2/3 localized near centromeres through meiosis, consistent with the PIAS1 immunostaining data and previous report (Feitosa et al, 2018). Furthermore, ratiometric analysis revealed that SUMO2/3 were enriched near centromeres at telophase I, similar to PIAS1 (Fig. 11, 17). Taken together, these data suggested that SUMO2/3 (referred to as centromeric SUMOs), but not SUMO1, are enriched at centromeres and that the enrichment is enhanced during post-anaphase-I periods.

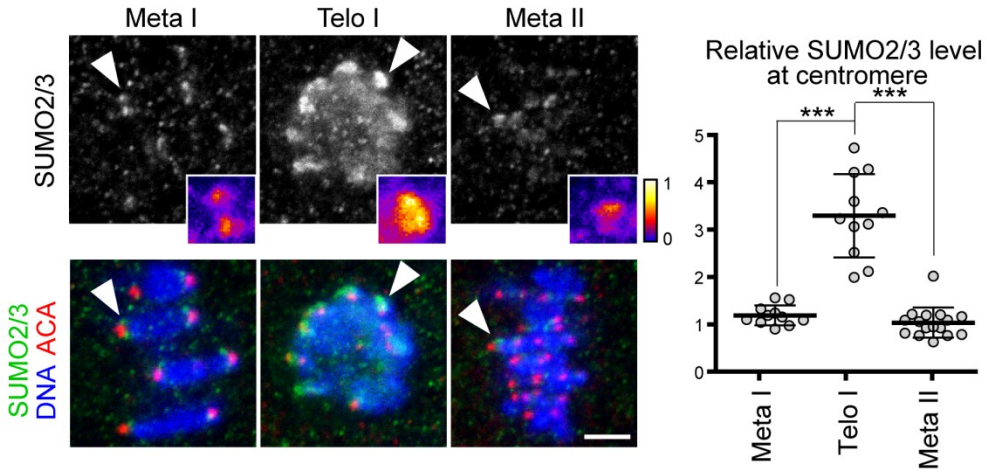

Fig. 17: Endogenous SUMO2/3 are enriched near centromeres at telophase I. Oocytes at metaphase I (4 hr after GVBD), telophase I (1.1 hr after anaphase I onset), and metaphase II (12-14 hr after GVBD) were stained for SUMO2/3 (green), centromeres (ACA, red), and DNA (Hoechst 33342, blue). The signals indicated with arrowheads

were magnified with fire color coding. Scale bar is 5 μm. The levels relative to ACA signals are shown (n = 11, 11, and 16 oocytes). Error bars show the SD. ***p<0.0001. (Ding *et al*, *Curr. Biol.* 2018)

3.4.3 SUMO2/3 are enriched near centromeres by covalent conjugation

To rule out the possibility that enrichment of mNG-SUMO2/3gg at telophase I is a non-covalent interaction, I made a non-conjugatable version of SUMO3 by replacing the last amino acid glycine with alanine (naming mNG-SUMO3ga). Then I microinjected mRNAs of mNG-SUMO3ga and H2B-mCherry into oocytes and checked whether this form of SUMO can localize near centromeres. As a control, I also injected same amount of mRNAs of mNG-SUMO3gg and H2B-mCherry into oocytes. mNG-SUMO3ga and mNG-SUMO3gg showed similar expression levels, as evidenced by the comparable signal intensities at the GV-stage. However, mNG-SUMO3ga failed to be enriched near centromeres at telophase I (Fig. 18). These results suggest that mNG-SUMO3gg localized near centromeres through covalent binding to the substrates.

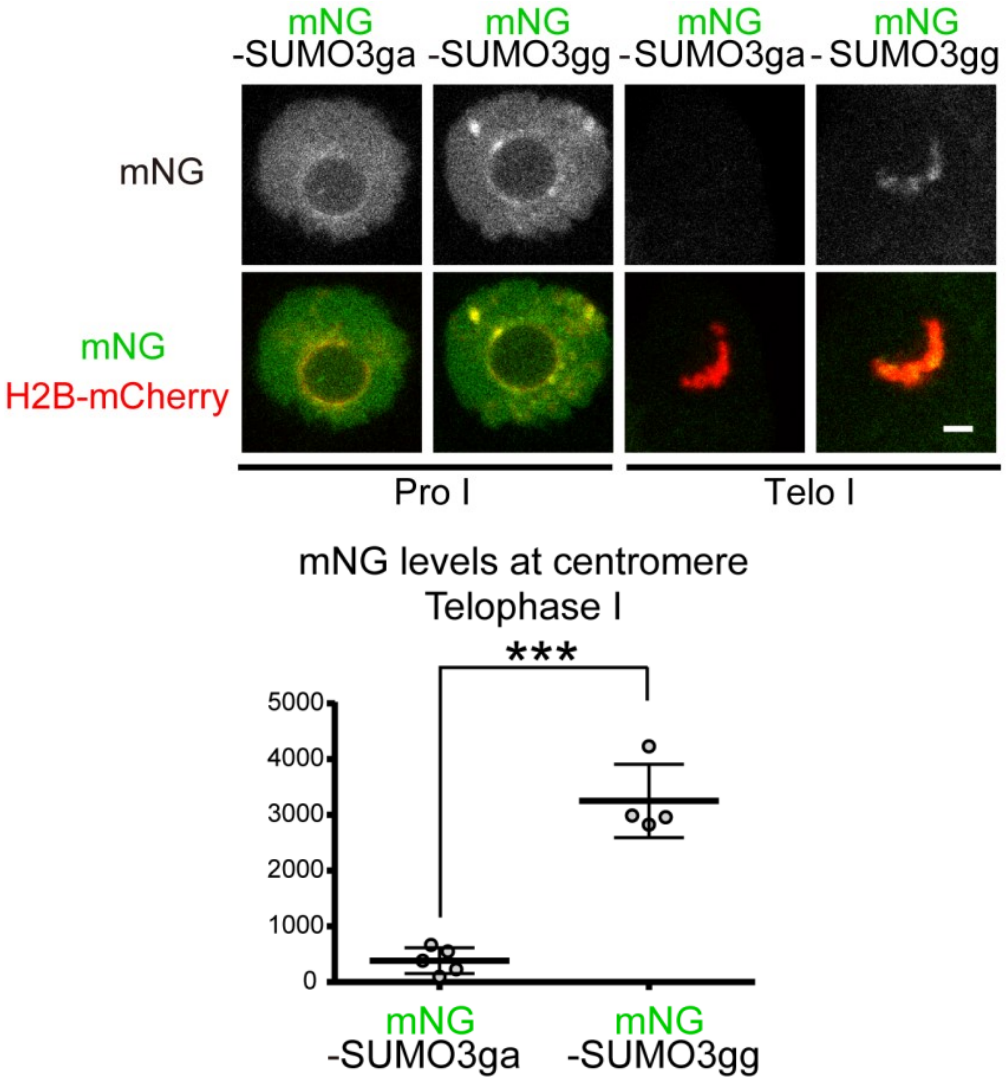

Fig. 18: mNG-SUMO3ga failed to be incorporated into sumoylation process at telophase I. Oocytes expressing mNG-SUMO3ga or -SUMO3gg (green) and H2B-mCherry (red) were imaged and analyzed. (n=5, 4 oocytes). Scale bar is 5 μm. Error bars show the SD. ***p<0.0001. (Ding *et al*, *Curr. Biol.* 2018)

3.5 Establishment of tools to inhibit sumoylation

3.5.1 Sumoylation inhibitor 2-D08 arrests cell cycle

To understand the functional importance of centromeric SUMO enhancement, I first evaluated the chemical inhibitor 2-D08 to manipulate sumoylation levels during meiosis. 2-D08 is a newly reported cell-permeable inhibitor, which blocks the E2 ligase activity without effects on global ubiquitination process in cultured cells (Kim et al. 2013). As there is only one E2 ligase in the mouse genome, 2-D08 acts as a global inhibitor for sumoylation.

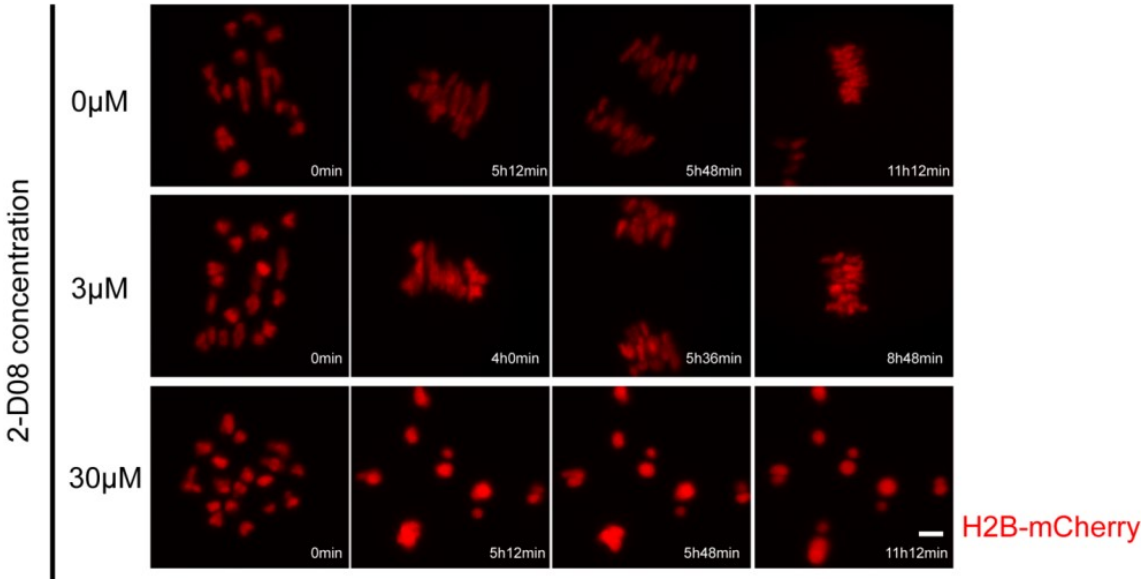

Fig. 19: 2-D08 treatment causes arrested cell cycle. Chromosomes are visualized by H2B-mCherry (red). 2-D08 was added to the cultures after GVBD, time was shown after drug administration (hr:min). Scale bar 5 μm.

I first tested the drug in series of different concentrations. H2B-mCherry was expressed in oocytes to label chromosomes. Because sumoylation is involved in GVBD, 2-D08 was added to the oocyte culture after GVBD. Live imaging data showed that chromosomes successfully congressed to the spindle equator, segregated into different

daughter cells and bioriented at metaphase II in control oocytes. However, in 30 μM 2-D08 treatment condition, cell cycle was arrested; furthermore, chromosomes were dispersed and lost dynamics, suggesting severe spindle defects (Fig. 19). However, if treated with 3 μM 2-D08, oocytes did not show any noticeable defects in terms of abnormal chromosomes or delayed anaphase I onset time (Fig. 19). I reasoned that defects in 30 μM 2-D08 treatment condition are not due to malfunction of centromeric sumoylation but the global sumoylation.

3.5.2 Tethering a dominant-negative PIAS1 can inhibit enrichment of centromeric sumoylation

Then I tested other strategy to specifically inhibit sumoylation near centromeres. SP-RING domain in PIAS1 is essential for E3 ligase activity. After replacing the amino acid cysteine-350 with serine (C350S)in SP-RING domain, this mutated version of PIAS1 can act as dominant-negative inhibitor for sumoylation both *in vivo* and *in vitro* (Liang et al. 2004; Yurchenko et al. 2006). Due to the high similarity between different PIAS proteins, this dominant-negative PIAS1 may also inhibit activities of all the PIAS proteins. I then made a construct with the same mutation, namely PIAS1(dn). To test whether PIAS1(dn) can localize near centromeres or not, I expressed mEGFP-PIAS1(dn) and H2B-mCherry in oocytes and checked its localization at 60 min after anaphase I onset. As a control, I also introduced mEGFP-PIAS1 and H2B-mCherry into GV-stage oocytes. However, mEGFP-PIAS1(dn) lost its ability to localize near centromeres at telophase I, indicating that sumoylation activity is necessary for PIAS1 localization (Fig. 20). I then checked the SUMO2/3 levels of mNG-PIAS1(dn) expressing oocytes at telophase I (1.1 hr after anaphase I) to examine

whether SUMO2/3 levels at centromeres can be inhibited at the expression level I used. I expressed mNG or mNG-PIAS1(dn) in oocytes fixed the oocytes and stained for SUMO2/3 and centromeres at telophase I. After quantification of centromeric SUMO2/3 levels relative to ACA levels, I did not observe any significant differences in centromeric SUMO2/3 levels in the two conditions (Fig. 20). These data suggested that cytoplasmic PIAS1(dn) at the concentration I tested was not adequate to inhibit sumoylation near centromeres.

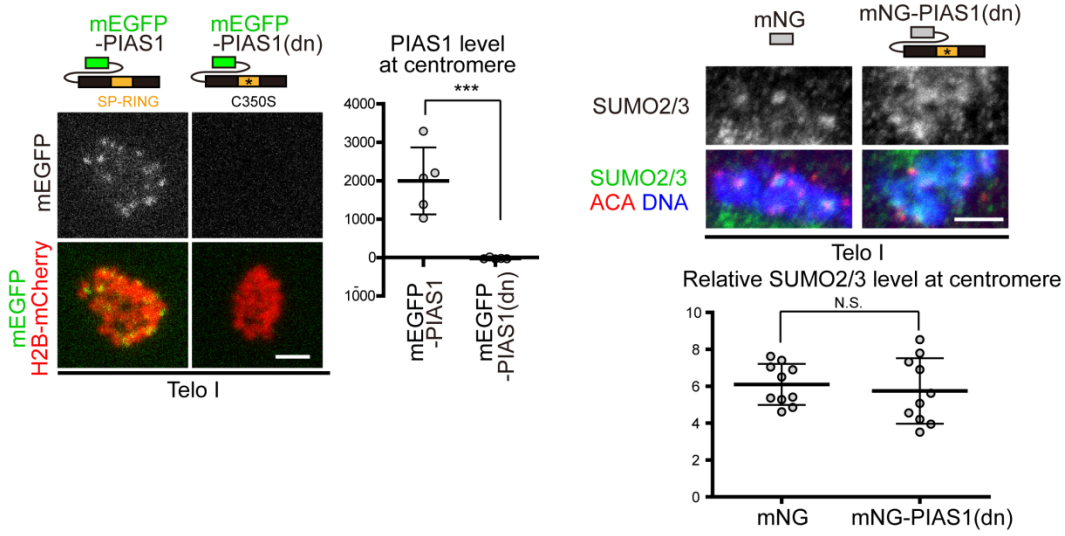

Fig. 20: PIAS1(dn) fails to localize near centromeres and perturb centromeric enrichment of SUMO2/3 at telophase I. Oocytes expressing mEGFP-PIAS1 or PIAS1(dn) (green) and H2B-mCherry (red) were imaged. Scale bar is 5 μm. The levels of mEGFP signals near centromeres were quantified at telophase I (60 min after anaphase I onset) (n=5, 5, 5 oocytes.). Error bars show the SD. ***P<0.0001. Oocytes expressing mNG or mNG-PIAS1(dn) were fixed at telophase I and stained for SUMO2/3 (green), centromeres (ACA, red) and DNA (Hoechst33342, blue). Scale bar is 5 μm.

The levels of SUMO2/3 signals relative to ACA signals were quantified (n=10, 10 oocytes). Error bars show the SD. N.S., not significant. (Ding *et al*, *Curr. Biol.* 2018)

I then expected that tethering PIAS1(dn) to centromeres may inhibit sumoylation by creating a locally concentrated PIAS1(dn). To test this idea, I created a CENP-C-fused PIAS1(dn) namely PIAS1(dn)-CENP-C. As a control, I also created PIAS1-CENP-C. Live imaging results confirmed that both mNG-PIAS1(dn)-CENP-C and mNG-PIAS1-CENP-C can be effectively targeted to centromeres (Fig. 21).

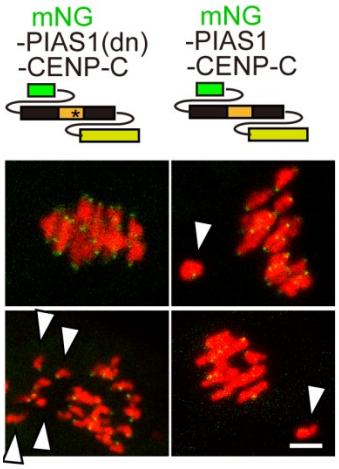

Fig. 21: mNG-PIAS1(dn)-CENP-C and mNG-PIAS1-CENP-C can localize at centromeres during meiosis. mNG-fused constructs (green) were expressed together with H2B-mCherry (red). Arrowheads indicate misaligned chromosomes. Scale bar is 5μm. (Ding *et al*, *Curr. Biol.* 2018)

So I then inspected the centromeric SUMO levels after expressing PIAS1(dn)-CENP-C or CENP-C in oocytes. I fixed the oocytes expressing PIAS1(dn)-CENP-C or CENP-C at telophase I and stained for SUMO2/3 and centromeres. As expected, in

PIAS1(dn)-CENP-C expressing oocytes, centromeric SUMO2/3 levels were significantly lower compared to control oocytes expressing CENP-C (Fig. 22). I also tested the PIAS1-CENP-C construct in oocytes and stained for SUMO2/3 at telophase I. Quantification of immunofluorescence showed that PIAS1-CENP-C can greatly enhance centromeric SUMO2/3 levels at telophase I (Fig. 22). In summary, I can utilize these tools to manipulate sumoylation specifically at centromeres. Furthermore, these results suggested that centromeric SUMO2/3 enrichment depends on PIAS proteins.

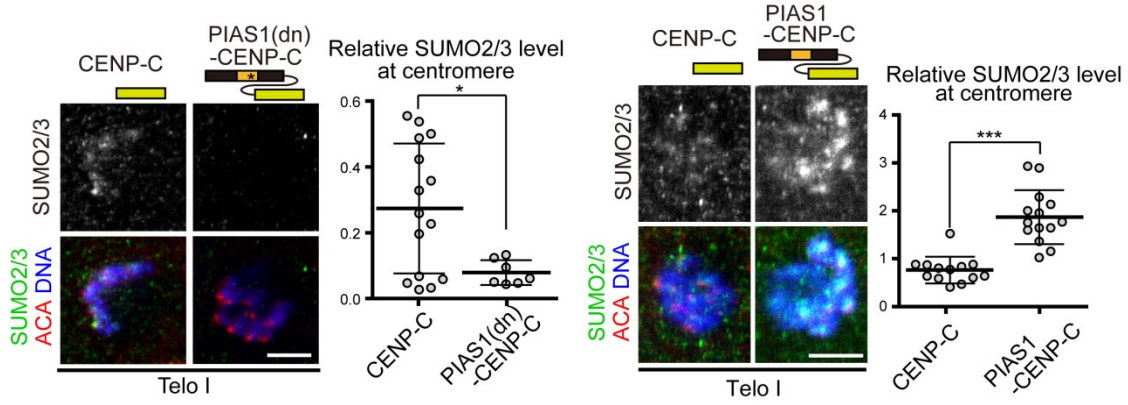

Fig. 22: Manipulations of SUMO2/3 enrichment near centromeres. Oocytes were fixed at telophase I (1.1 hr after anaphase I onset) and stained for SUMO2/3 (green), kinetochores (ACA, red), and DNA (Hoechst 33342, blue). The levels of SUMO2/3 signals relative to ACA signals were quantified (n = 15 and 7 oocytes for PIAS1(dn)-CENP-C experiment, n = 13 and 14 oocytes for PIAS1-CENP-C experiment). Scale bar is 5 μm. Error bars show the SD. *P<0.05, ***P<0.0001. (Ding *et al*, *Curr. Biol.* 2018)

3.6 Inhibition of sumoylation causes precocious cohesion lost at meiosis II

3.6.1 Inhibition of centromeric sumoylation causes misaligned chromosomes at meiosis II

To check phenotypes after inhibition of centromeric sumoylation, I expressed mNG-CENP-C, mNG-PIAS1(dn), mNG-PIAS1(dn)-CENP-C or mNG-PIAS1-CENP-C and H2B-mCherry in oocytes and monitored the dynamics of chromosomes by live imaging. Live imaging data revealed that in control oocytes expressing mNG-CENP-C, chromosomes were congressed and bioriented at the spindle equator at both metaphase I and metaphase II (Fig. 23). Consistent with the fact that mNG-PIAS1(dn) did not affect centromeric sumoylation enrichment, oocytes expressing mNG-PIAS1(dn) showed no obvious defects in chromosome dynamics during meiosis process (Fig. 23). However, in mNG-PIAS1(dn)-CENP-C-expressing oocytes, there were massive misaligned chromosomes at metaphase II while metaphase I was relatively normal (Fig. 23). In contrast, there were misaligned chromosomes at both metaphase I and metaphase II in mNG-PIAS1-CENP-C expressing oocytes (Fig. 23), which was possibly due to kinetochore-microtubule attachment errors in mNG-PIAS1-CENP-C expressing oocytes.

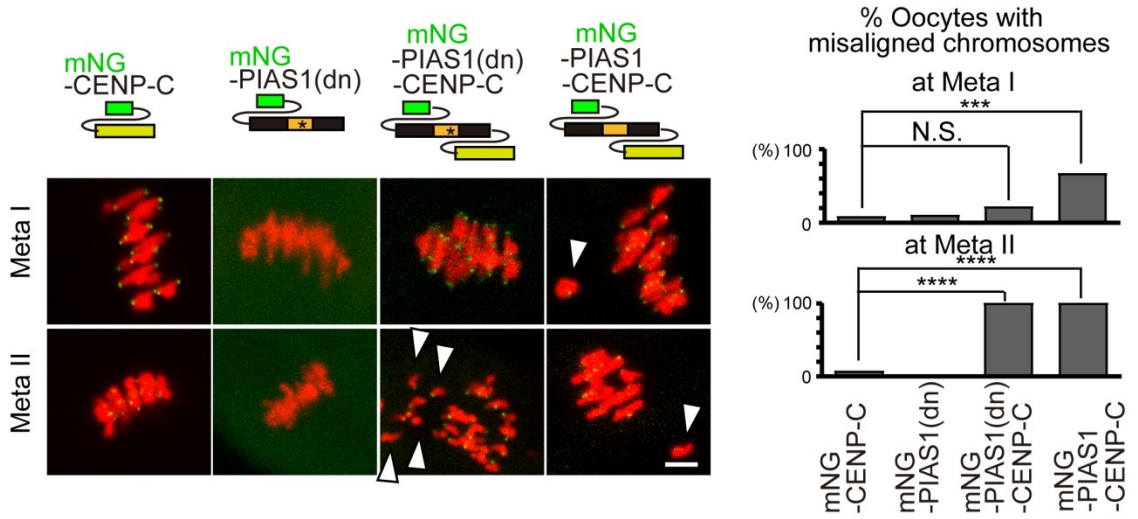

Fig. 23: PIAS1(dn)-CENP-C causes chromosome misalignment at meiosis II. mNG-fused constructs (green) were expressed together with H2B-mCherry (red). Arrowheads indicate misaligned chromosomes. Scale bar is 5μm.Oocytes with misaligned chromosomes at metaphase I (5 hr after GVBD) and metaphase II (12–14 hr after GVBD) were scored (n = 13, 10, 7, and 18 oocytes). Fisher's exact test was used. N.S. no significance, ***p < 0.001, ****p < 0.0001. (Ding *et al*, *Curr. Biol.* 2018)

3.6.2 Inhibition of centromeric sumoylation causes precocious cohesion lost at meiosis II

To further understand how chromosomes were misaligned at meiosis II in mNG-PIAS1(dn)-CENP-C-expressing oocytes, I fixed the oocytes expressing CENP-C, PIAS1(dn)-CENP-C or PIAS1-CENP-C at 12-14 hr after GVBD, stained for centromeres and chromosomes. After 3D reconstruction in Imaris, I designated sister kinetochores by minimizing sister kinetochore distances and the angles between the spindle axis and the axis connecting the sister kinetochore pair. Sister kinetochore distances were then calculated and used as indicators for cohesion defects (see material and methods). This

analysis confirmed that centromeric cohesion was intact in CENP-C expressing oocytes. However, centromeric cohesion was severely impaired in oocytes expressing PIAS1(dn)-CENP-C indicated by a large number of separated sister chromatids. Although massive misaligned chromosomes were observed in PIAS1-CENP-C expressing oocytes, most of them were still intact in cohesion (Fig. 24). In conclusion, centromeric SUMO enrichment is needed for cohesion protection during meiosis.

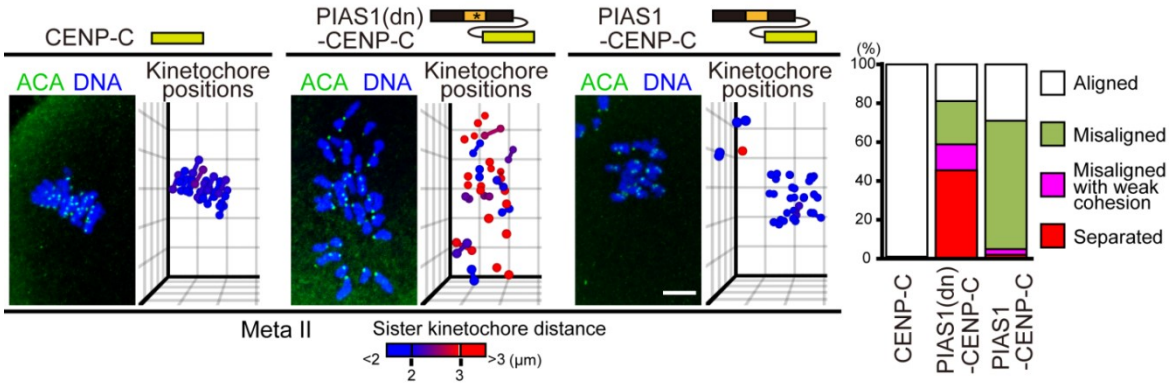

Fig. 24: PIAS1(dn)-CENP-C causes cohesion defects. Oocytes were fixed at metaphase II (12–14 hr after GVBD) and stained for centromeres (ACA, green) and DNA (Hoechst 33342, blue). Scale bar is 5μm. In the 3D plots, kinetochore positions are indicated by spheres. Sister kinetochores that exhibited an inter kinetochore distance <3 μm are connected by lines. The color code indicates the inter kinetochore distance. Unit of the grid is 5 μm. Kinetochore pairs were categorized based on inter kinetochore distance and alignment (n = 100, 180, and 100 pairs of 5, 9, and 5 oocytes). (Ding *et al*, *Curr. Biol.* 2018)

3.6.3 Inhibition of centromeric sumoylation causes precocious loss of cohesin

The cohesin complex is the mediator of cohesion, so I also checked whether the cohesin complex was intact or not in PIAS1(dn)-CENP-C-expressing oocytes. Rec8 is a meiosis-specific cohesin component, which is cleaved along the chromosome arms but remained intact at centromeres at anaphase I onset. In order to detect robust immunofluorescent signals, I microinjected Rec8 antibody into live oocytes at 12-14 hr after GVBD and then fixed the oocytes and stained for Rec8 and centromeres. In oocytes expressing CENP-C, I succeeded in detecting Rec8 signals between sister kinetochores. However, oocytes expressing PIAS1(dn)-CENP-C lost Rec8 signals at metaphase II (Fig. 25). Then I tested whether the cohesin complex was intact at telophase I. After expressing PIAS1(dn)-CENP-C or CENP-C, I fixed oocytes at telophase I and then stained for SMC3, which is another cohesin component, and centromeres. As expected, SMC3 signals were detected between sister kinetochores in control oocytes expressing CENP-C (Fig. 26). However, SMC3 protein levels were significantly decreased at telophase I in oocytes expressing PIAS1(dn)-CENP-C (Fig. 26). These data suggested that cohesin complex was lost in PIAS1(dn)-CENP-C expressing oocytes at telophase I and metaphase II. Thus, centromeric sumoylation enrichment is required for cohesin protection in meiosis.

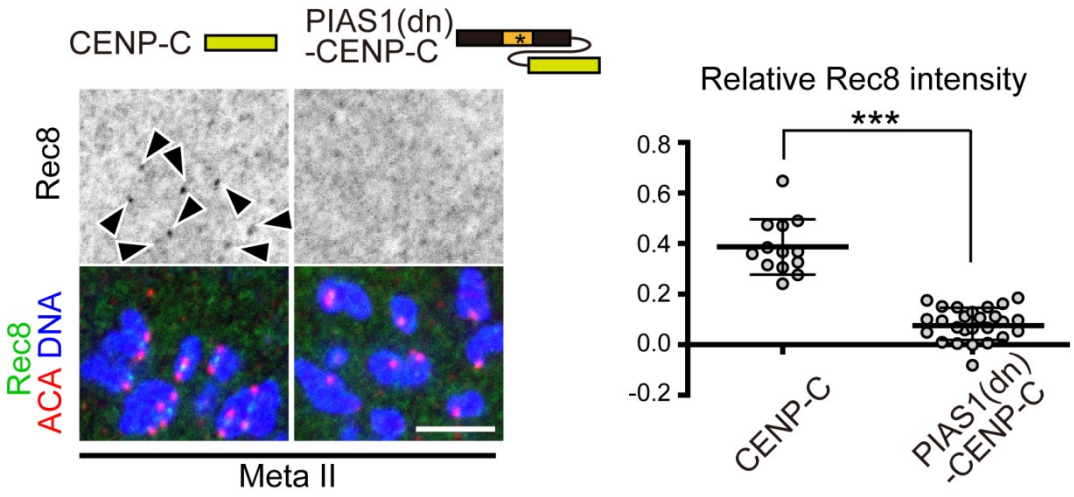

Fig. 25: PIAS1(dn)-CENP-C causes loss of centromeric cohesin. Oocytes were fixed at metaphase II (12–14 hr after GVBD) and stained for Rec8 (green), centromeres (ACA, red), and DNA (Hoechst 33342, blue). Arrowheads indicate centromeric Rec8 signals. Scale bar is 5 μm. The levels of Rec8 signals relative to ACA signals were quantified (n = 13 and 26 oocytes). Error bars show the SD. ***p < 0.001. (Ding *et al*, *Curr. Biol.* 2018)

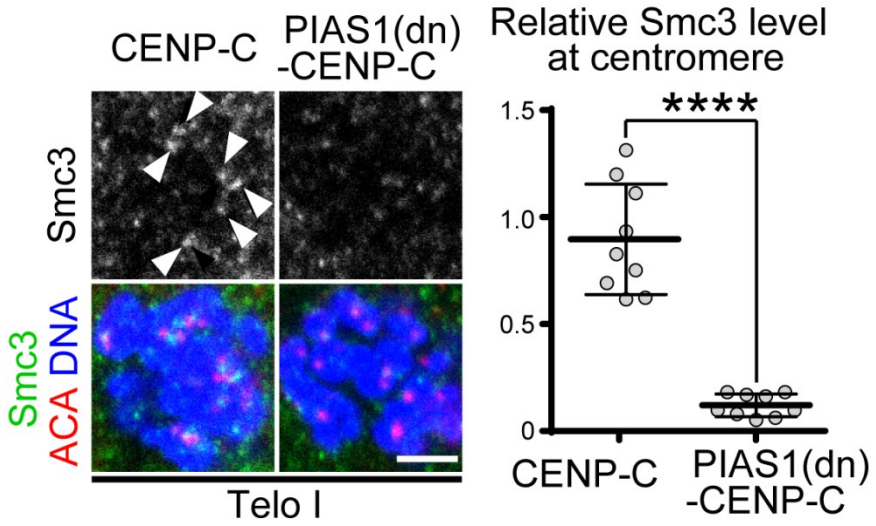

Fig. 26: PIAS1(dn)-CENP-C causes precocious loss of centromeric Smc3. Oocytes expressing PIAS1(dn)-CENP-C or CENP-C were fixed at telophase I (1.1 h after anaphase I onset) and stained for Smc3 (green), centromeres (ACA, red), and DNA (Hoechst33342, blue). Arrowheads indicate centromeric Smc3 signals. Scale bar is 5 μm. The levels of Smc3 signals relative to ACA signals are shown (n=9, 9 oocytes). Error bars show the SD. ****P<0.0001. (Ding *et al*, *Curr. Biol.* 2018)

3.7 PIAS1(dn)-CENP-C-expressing oocytes are proficient in Sgo2-dependent protection

3.7.1 Inhibition of centromeric sumoylation down regulates Sgo2 levels at centromeres

Sgo2 plays a key role in centromeric cohesion protection during meiosis in mammals. Although centromeric Sgo2 sharply decreased at anaphase I onset and was undetectable after anaphase I, it was still not clear whether Sgo2 was involved in sumoylation-dependent centromeric cohesion protection in meiosis. I evaluated Sgo2 protein levels at centromeres in wild-type oocytes expressing PIAS1(dn)-CENP-C or CENP-C and *Sgo2*+/- oocytes expressing CENP-C. These oocytes were fixed at 4 hr after GVBD, and stained for Sgo2 and centromeres. Sgo2 levels relative to ACA levels were quantified. Quantifications showed that in *Sgo2*+/- oocytes, there was a half amount of Sgo2 proteins at centromeres compared to wild-type oocytes. Meanwhile, wild-type oocytes expressing PIAS1(dn)-CENP-C only retained a half amount of Sgo2 compared with wild-type oocytes expressing CENP-C, which was comparable to that in

Sgo2+/- oocytes expressing CENP-C (Fig. 27). It was clear that PIAS1(dn)-CENP-C also down regulated Sgo2 levels at centromeres.

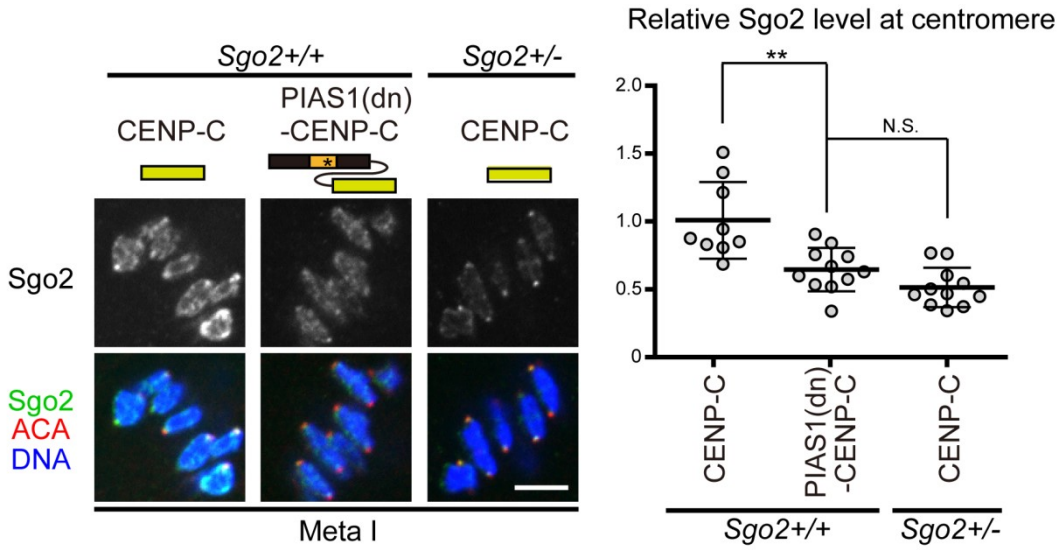

Fig. 27: PIAS1(dn)-CENP-C-expressing oocytes have similar Sgo2 levels at centromeres as *Sgo2*+/− oocytes. Oocytes were fixed at metaphase I (4 hr after GVBD) and stained for Sgo2 (green), kinetochores (ACA, red), and DNA (Hoechst 33342, blue). The levels of Sgo2 signals relative to ACA signals were shown (n = 9, 11, and 11 oocytes). Scale bar is 5μm. Error bars show the SD. **P<0.001, N.S. not significant. (Ding *et al*, *Curr. Biol.* 2018)

3.7.2 Decreased Sgo2 localization in PIAS1(dn)-CENP-C expressing oocytes does not account for precocious cohesion loss at meiosis II

To test the possibility that halved amount of Sgo2 level at centromeres in PIAS1(dn)-CENP-C was the reason for centromeric cohesion defects at metaphase II, I allowed wild-type oocytes expressing PIAS1(dn)-CENP-C or CENP-C and *Sgo2*+/-

oocytes expressing CENP-C to mature, fixed these oocytes at 12-14 hr after GVBD and stained for centromeres and chromosomes. High resolution 3D reconstructions of kinetochores and chromosomes were done and analyzed by the same way above (Fig. 24). The results showed that in *Sgo2*+/- oocytes, the cohesion was still intact as wild-type oocytes (Fig. 28), suggesting that even with a half amount of Sgo2 proteins at centromeres, oocytes were still capable to maintain centromeric cohesion until metaphase II. However, wild-type oocytes expressing PIAS1(dn)-CENP-C with half amount of Sgo2 still showed massive precocious segregation of sister chromatids at metaphase II (Fig. 28). These data demonstrated that a decreasing in centromeric Sgo2 does not account for precocious centromeric cohesion loss in PIAS1(dn)-CENP-C-expression oocytes. Thus, centromeric sumoylation plays a role in cohesion protection independently of Sgo2.

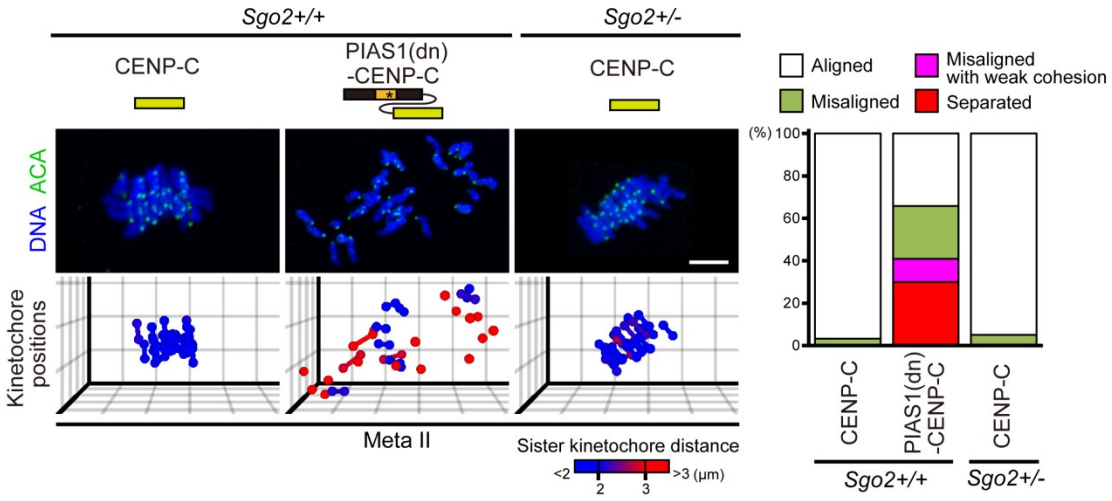

Fig. 28: Cohesion defects in PIAS1(dn)-CENP-C-expressing oocytes are not attributable to reduced Sgo2. Oocytes were fixed at metaphase II (12–14 hr after GVBD) and stained for kinetochores (ACA, green) and DNA (Hoechst 33342, blue).

Scale bar is 5 μm. In the 3D plots, kinetochore positions are indicated by spheres. Sister kinetochores that exhibited an inter kinetochore distance <3 μm are connected by lines. The color code indicates inter kinetochore distance. Unit of the grid is 5 μm. Kinetochore pairs were categorized based on inter kinetochore distance and alignment (n = 120, 120, and 160 pairs of 6, 6, and 8 oocytes). (Ding *et al*, *Curr. Biol.* 2018)

3.7.3 PIAS1(dn)-CENP-C-expressing oocytes are proficient in Sgo2-dependent protection

Separase reaches maximum activity at anaphase I onset, when Sgo2 counteracts separase activity. In *Sgo2* knockout oocytes, sister kinetochores were immediately separated after anaphase I onset. If centromeric sumoylation played a role in cohesion protection independently of Sgo2, it would be expected that oocytes expressing mNG-PIAS1(dn)-CENP-C sustained intact centromeric cohesion immediately after anaphase I onset. To test this idea, I implemented high spatial-temporal resolution live imaging and kinetochore tracking to monitor sister kinetochore distances. Wild-type oocytes expressing mNG-CENP-C or mNG-PIAS1(dn)-CENP-C and *Sgo2*-/- oocytes expressing mNG-CENP-C and H2B-mCherry were imaged before anaphase I onset. In a 2-min time interval tracking, I succeed in tracking nearly all sister kinetochores in *Sgo2* knockout oocytes expressing mNG-CENP-C and wild-type oocytes expressing mNG-CENP-C or mNG-PIAS1(dn)-CENP-C. Before anaphase I onset, there were no differences in the sister kinetochore distances in all groups. In mNG-CENP-C-expressing wild-type oocytes, average sister kinetochore distance was 0.63±0.04 μm at 6 min after anaphase I onset, suggesting intact centromeric cohesion. *Sgo2* knockout oocytes showed significantly increased average distance of sister

kinetochores at 6 min (1.34±0.35 μm), which is consistent with the previous report (Llano et al., 2008). Remarkably, there was no significant difference in average sister kinetochore distance between wild-type oocytes expressing mNG-PIAS1(dn)-CENP-C (0.74±0.19 μm) and CENP-C at 6 min after anaphase I onset (Fig. 29). These results suggested that mNG-PIAS1(dn)-CENP-C expressing oocytes were proficient in Sgo2-dependent centromeric cohesion protection during anaphase I onset.

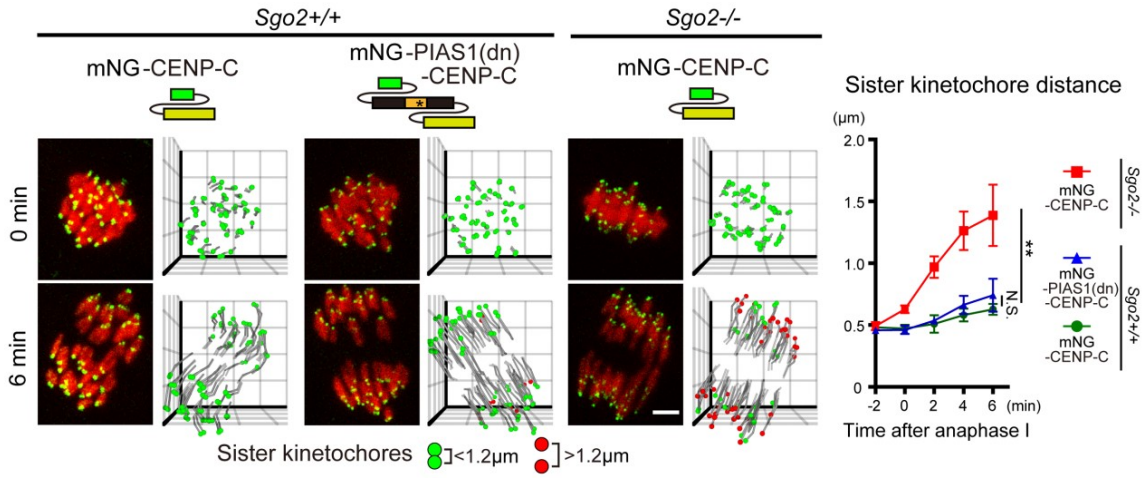

Fig. 29: PIAS1(dn)-CENP-C-expressing oocytes are proficient in Sgo2-dependent protection. *Sgo2*+/+ and *Sgo2*−/− oocytes expressing mNG-CENP-C or mNG-PIAS1(dn)-CENP-C (green) and H2B-mCherry (red) were imaged around anaphase I onset. Kinetochore signals were processed for peak enhancement and background subtraction. Kinetochore trajectories are shown in 3D plots. Sister kinetochores exhibiting >1.2-μm inter kinetochore distance are represented by red spheres, whereas the others are represented by green spheres. Unit of the grid is 5 μm. Distances of sister kinetochores are plotted over time (n = 4, 4, and 3 oocytes). Error bars show the SD. **P<0.001, N.S. no significances. (Ding *et al*, *Curr. Biol.* 2018)

3.8 Post-anaphase-I sumoylation is required for centromeric cohesion protection

3.8.1 Development of a cleavable form of PIAS1(dn)-CENP-C

As centromeric SUMOs are progressively enriched after anaphase I and reached maximum at ~80 min after anaphase I onset, I speculated that sumoylation-dependent cohesion protection during post-anaphase-I periods was required for centromeric cohesion maintenance. However, the tools I used above were continuously inhibiting centromeric sumoylation. If inhibition of centromeric sumoylation is removed after anaphase I onset, it would be expected that the cohesion defects would be largely relieved. To develop a cleavable form of PIAS1(dn)-CENP-C, I utilized the fact that cohesin component Rec8 is cleaved by separase, which is sharply activated at anaphase I onset (Kudo et al. 2009; Shindo et al. 2012). To evaluate the cleavage efficiency, I inserted a Rec8 fragment (227-484 amino acids) between mEGFP and mCherry, which was targeted to centromeres by fusing with CENP-C (mEGFP-Rec8f-mCherry-CENP-C). Meanwhile, three cleavage sites of the Rec8f were mutated into a resistant form as a control, namely mEGFP-Rec8f(nc)-mCherry-CENP-C. I expressed mEGFP-Rec8f-mCherry-CENP-C or mEGFP-Rec8f(nc)-mCherry-CENP-C in oocytes, and imaged them before anaphase I onset. Ratio between mEGFP and mCherry signal intensity was calculated and plotted. The plot showed that before anaphase I onset, both two constructs showed constant mEGFP/mCherry ratio, demonstrating that there was no precocious cleavage of the Rec8 fragments. The cleavable mEGFP-Rec8f-mCherry-CENP-C showed a sharp cleavage of the Rec8f at anaphase I onset (Fig.30). In contrast, non-cleavable mEGFP-Rec8f(nc)-mCherry-CENP-C showed no cleavage of Rec8f(nc). At 15 min after

anaphase I onset, there were significant differences in cleavage efficiency between non-cleavable and cleavable Rec8 fragments. These results showed that the Rec8f can be efficiently cleaved at anaphase I onset.

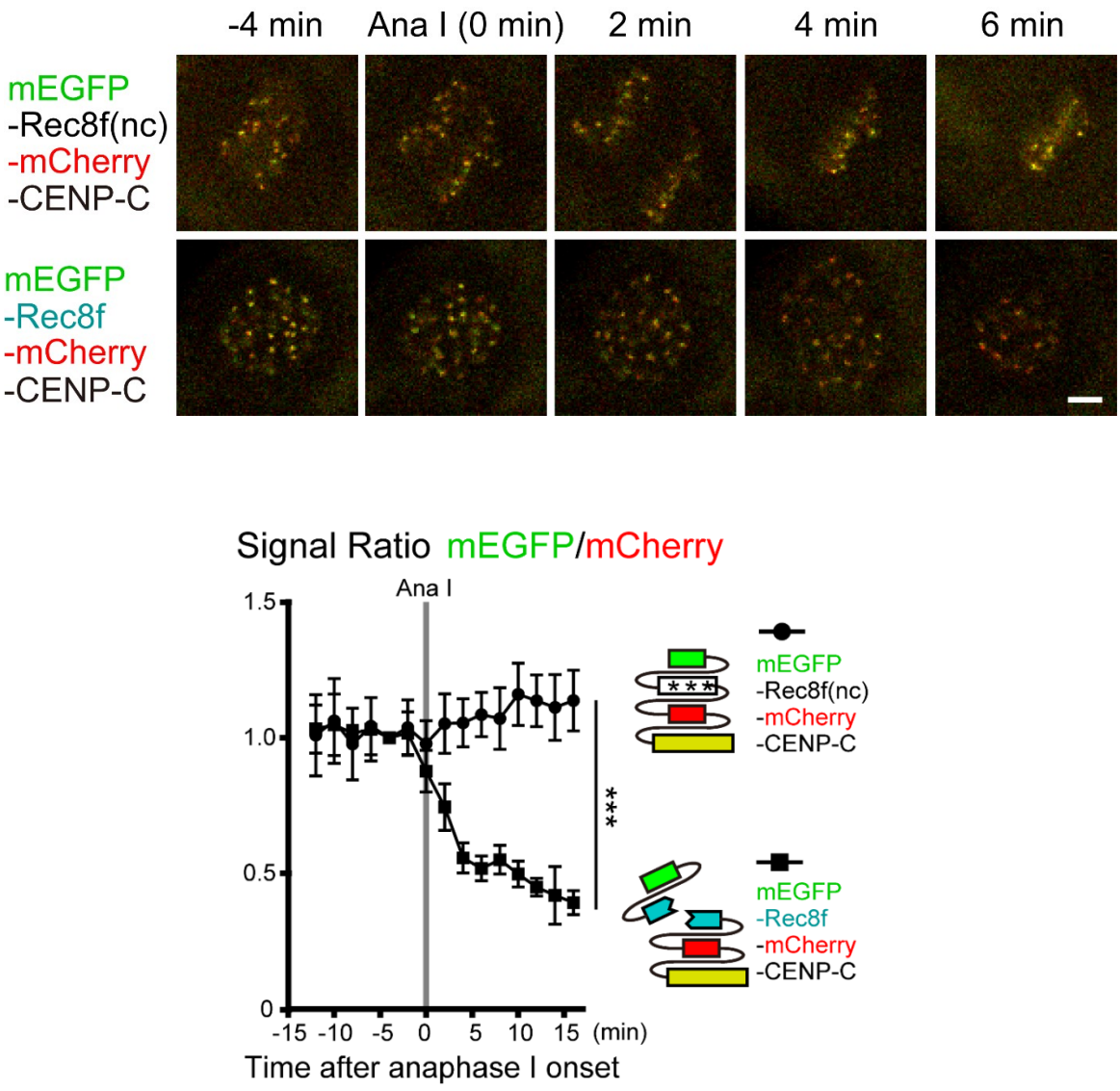

Fig. 30: Centromere-targeted Rec8f is cleaved at anaphase I. Oocytes expressing mEGFP-Rec8f-mCherryCENP-C or mEGFP-Rec8f(nc)-mCherry-CENP-C were imaged around anaphase I onset. Scale bar is 5 µm. The centromeric levels of mEGFP signals relative to mCherry signals were quantified and plotted (n=5, 5 oocytes). Error bars

show the SD. ***P<0.0001. (Ding *et al*, *Curr. Biol.* 2018)

Having proved that Rec8f is sharply cleaved at anaphase I onset, I inserted the fragment between PIAS1(dn) and CENP-C to cancel the sumoylation inhibition after anaphase I onset. I made a mNG-tagged version to evaluate the cleavage of PIAS1(dn)-Rec8f-CENP-C. As a control, I also expressed the non-cleavable form mNG-PIAS1(dn)-Rec8f(nc)-CENP-C in oocytes. I monitored the mNG signal intensity by live imaging. Consistently, mNG-PIAS1(dn)-Rec8f-CENP-C exhibited significantly decreased centromeric localization at telophase I compared to mNG-PIAS1(dn)-Rec8f(nc)-CENP-C, although they had similar expression levels at metaphase I (Fig. 31). This result showed that in mNG-PIAS1(dn)-Rec8f-CENP-C expressing oocytes, a large fraction of mNG-PIAS1(dn)-CENP-C was removed from centromeres at anaphase I onset.

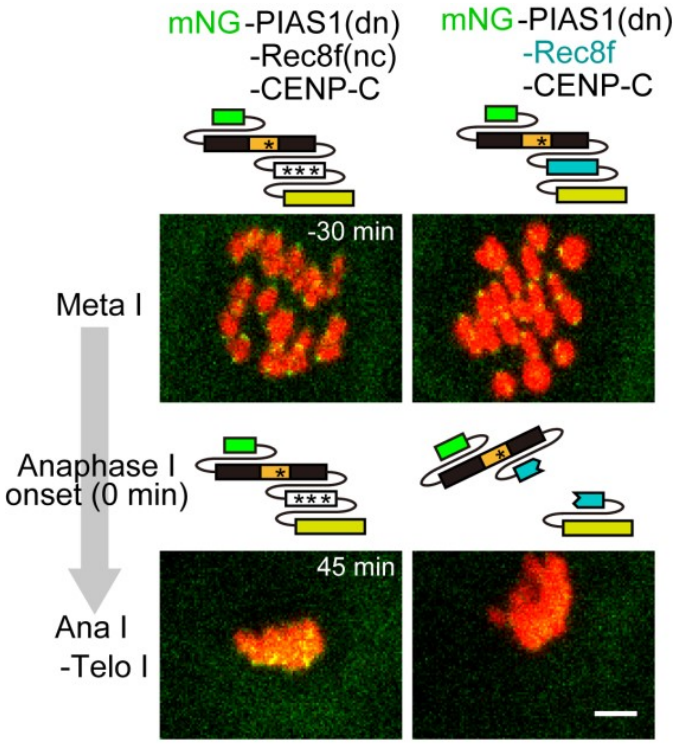

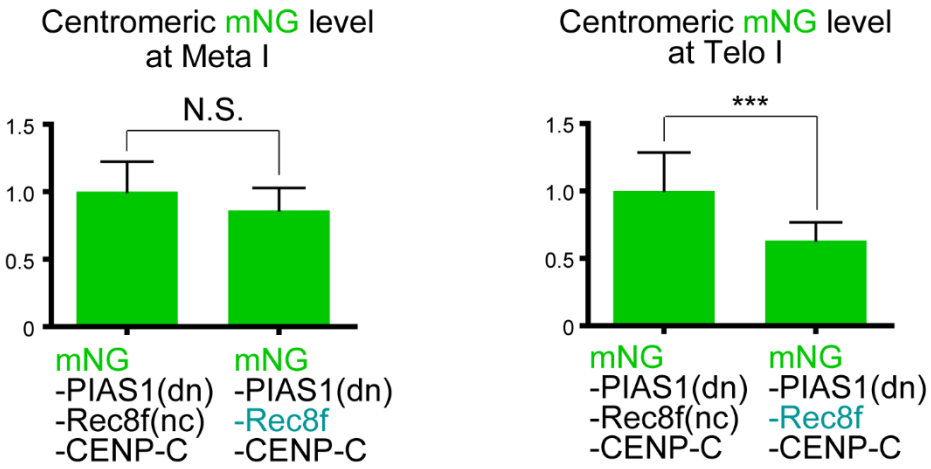

Fig. 31: Cleavage of mNG-PIAS1(dn)-Rec8f-CENP-C reduces its centromeric levels during post-anaphase-I periods. The centromeric levels of mNG signals were quantified 6 hr after nuclear envelope breakdown (NEBD) (Meta I) and 50 min after anaphase I onset (Telo I). Scale bar is 5 μm. Normalized values are shown (n = 7 and 7 oocytes). Error bars show the SD. N.S., not significant. ***P<0.0001. (Ding *et al*, *Curr. Biol.* 2018)

3.8.2 Cleavage of PIAS1(dn)-CENP-C at anaphase I onset largely rescued sumoylation levels at telophase I

Since I confirmed that PIAS1(dn)-Rec8f-CENP-C can be effectively removed from centromeres after anaphase I, I speculated that inhibition of centromeric sumoylation at telophase I should be largely restored. To test this, I introduced PIAS1(dn)-Rec8f-CENP-C into oocytes, fixed them at telophase I and stained for SUMO2/3 and centromeres. As a control, PIAS1(dn)-Rec8f(nc)-CENP-C was also expressed in oocytes. After quantifying relative SUMO2/3 levels at telophase I, I found that PIAS1(dn)-Rec8f-CENP-C expressing oocytes exhibited significantly higher centromeric SUMO2/3 levels than oocytes expressing PIAS1(dn)-Rec8f(nc)-CENP-C

(Fig. 32), suggesting that cleavage of the PIAS1(dn)-CENP-C from centromeres relieved inhibition of SUMO2/3 enrichment at telophase I.

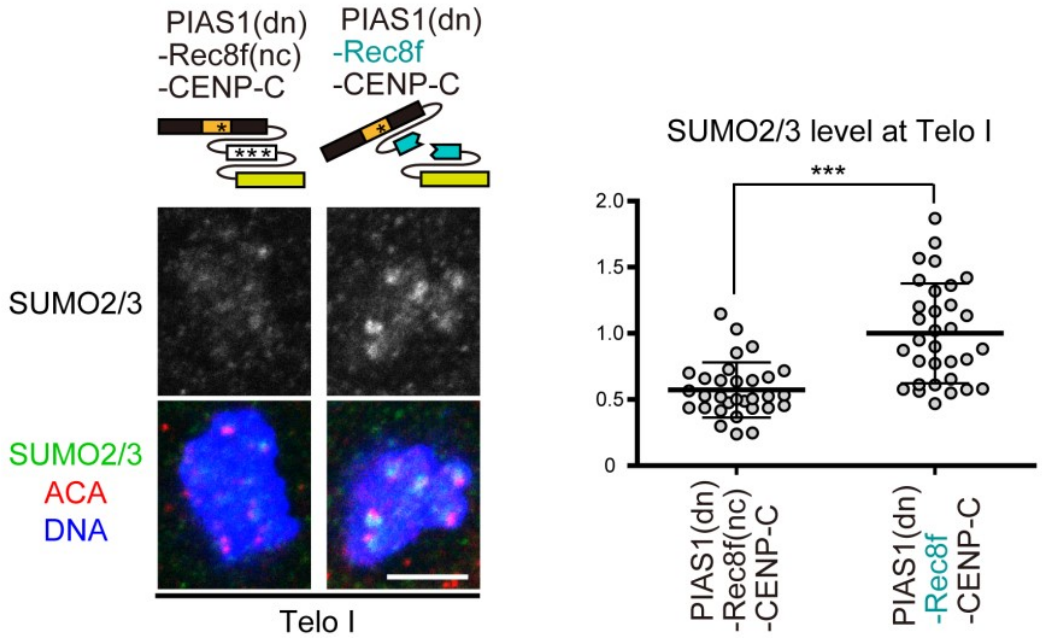

Fig. 32: Cleavage of PIAS1(dn)-Rec8f-CENP-C rescues centromeric SUMO2/3. Oocytes expressing PIAS1(dn)-Rec8f-CENP-C or non-cleavable PIAS1(dn)-Rec8f(nc)-CENP-C were fixed at telophase I (1.1 hr after anaphase I onset) and stained for SUMO2/3 (green), centromeres (ACA, red) and DNA (Hoechst33342, blue). Scale bar is 5 μm. The levels of SUMO2/3 signals relative to ACA signals are quantified and shown after normalization (n=31, 32 oocytes). Error bars show the SD. ***P<0.0001. (Ding *et al*, *Curr. Biol.* 2018)

3.8.3 Cleavage of PIAS(dn)-CENP-C at anaphase I onset rescued defective chromosome misalignment at metaphase II

Rescued centromeric SUMO2/3 levels in PIAS1(dn)-Rec8f-CENP-C expressing oocytes

is expected to alleviate defects at meiosis II. To test this, I checked chromosome alignment at metaphase II after expressing mNG-PIAS1(dn)-Rec8f-CENP-C or mNG-PIAS1(dn)-Rec8f(nc)-CENP-C in oocytes. In mNG-PIAS1(dn)-Rec8f(nc)-CENP-C expressing oocytes, there was a substantial fraction of oocytes exhibited misaligned chromosomes, consistent with the observation in PIAS1(dn)-CENP-C expressing oocytes (Fig. 23). Moreover, in oocytes expressing mNG-PIAS1(dn)-Rec8f-CENP-C, it was less frequent to observe misaligned chromosomes than mNG-PIAS1(dn)-Rec8f(nc)-CENP-C expressing oocytes (Fig. 33). Thus, canceling the inhibition of sumoylation after anaphase I rescued the chromosome misalignment defects.

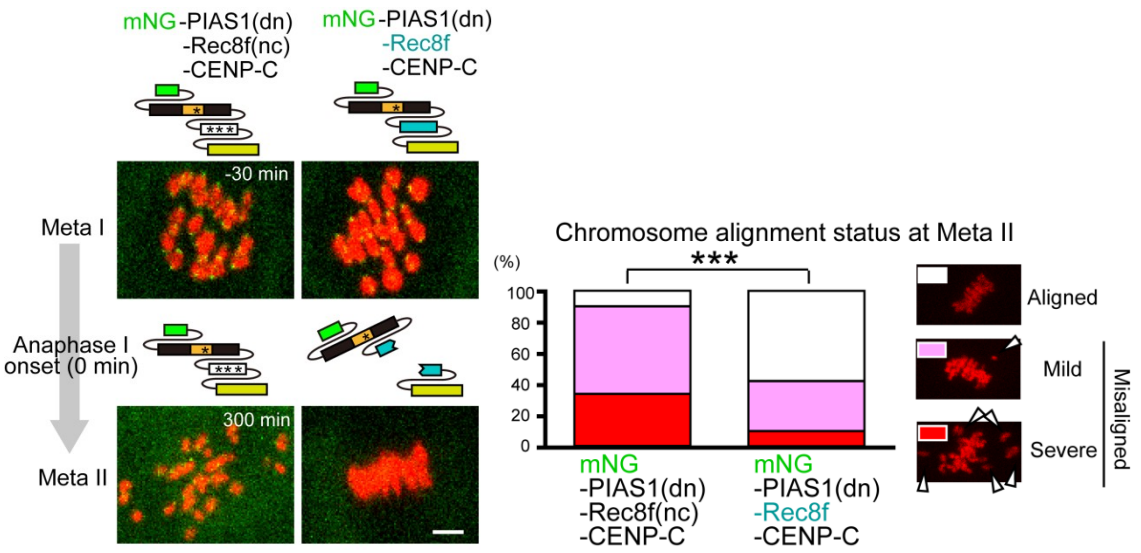

Fig. 33: Removal of PIAS1(dn) from centromeres at anaphase I suppresses chromosome misalignment at metaphase II. At metaphase II (6 hr after anaphase I onset), oocytes were categorized based on the number of misaligned chromosomes (n = 72 and 66 oocytes). Arrowheads indicate misaligned chromosomes. The Mann–Whitney U test was used. ***P<0.0001. (Ding *et al*, *Curr. Biol.* 2018)

3.8.4 Cleavage of PIAS(dn)-CENP-C at anaphase I onset rescued precocious separation of sister chromatids at metaphase II

To understand the reason of chromosome misalignment defects in mNG-PIAS1(dn)-Rec8f(nc)-CENP-C expressing oocytes, I expressed the cleavable or non-cleavable form of PIAS1(dn)-CENP-C, fixed the oocytes at metaphase II and did high resolution 3D reconstructions for kinetochores and chromosomes as above (Fig. 24, 28). Consistently, in PIAS1(dn)-Rec8f-CENP-C expressing oocytes, there were less precociously separated sister chromatids compared to PIAS1(dn)-Rec8f(nc)-CENP-C expressing oocytes (Fig. 34). These data suggested that removal of PIAS1(dn)-Rec8f-CENP-C at anaphase I onset restored the capacity of cohesion maintenance (Fig. 34), which rescued chromosome misalignment defects at metaphase II (Fig. 33). Thus, post-anaphase-I sumoylation enrichment is required for cohesion maintenance in meiosis.

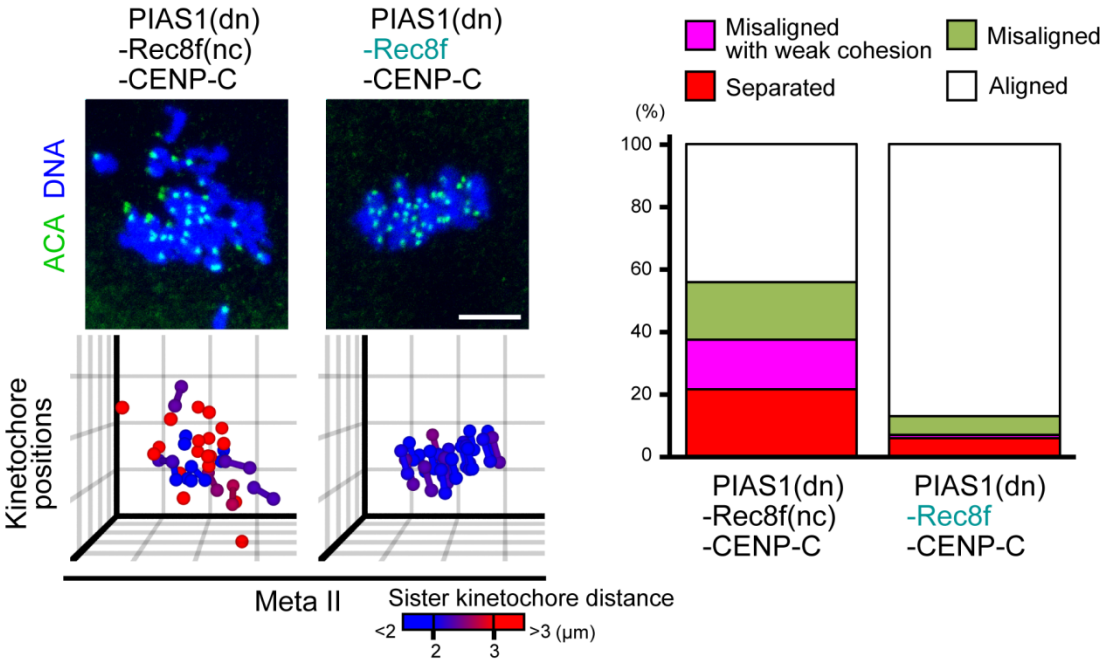

Fig. 34: Removal of PIAS1(dn) from centromeres at anaphase I suppresses cohesion defects at metaphase II. Oocytes were fixed at metaphase II (12–14 hr after GVBD) and stained for kinetochores (ACA, green) and DNA (Hoechst 33342, blue). Scale bar is 5 μm. In the 3D plots, kinetochore positions are indicated by spheres. Sister kinetochores that exhibited an inter kinetochore distance <3 μm are connected by lines. The color code indicates the inter kinetochore distance. Unit of the grid is 5 μm. Kinetochore pairs were categorized based on inter kinetochore distance and alignment (n = 100 and 100 pairs from 5 and 5 oocytes). (Ding *et al*, *Curr. Biol.* 2018)

3.9. Tests for possible targets of SUMO-dependent cohesion protection pathway during post-anaphase-I stages

3.9.1 PIAS1(dn)-CENP-C does not cause cohesion defects in meiosis II egg

The Wapl pathway contributes to chromosome cohesion disassociation during prophase in mitosis. A report showed that sumoylation of Scc1 opposes Wapl function in HeLa cells (Wu et al, 2012). It is possible that centromeric sumoylation counteracts Wapl activity to maintain cohesion during post-anaphase-I periods. If this holds true, inhibition of centromeric sumoylation at meiosis II should cause centromeric cohesion defects. To test this idea, I expressed PIAS1(dn)-CENP-C at meiosis II egg and analyzed the sister kinetochore distances by 3D reconstruction of kinetochores and chromosomes. The result showed that PIAS1(dn)-CENP-C did not cause detectable defects on centromeric cohesion during meiosis II (Fig. 35). These results made it unlikely that the centromeric sumoylation maintains centromeric cohesion through antagonizing Wapl activity.

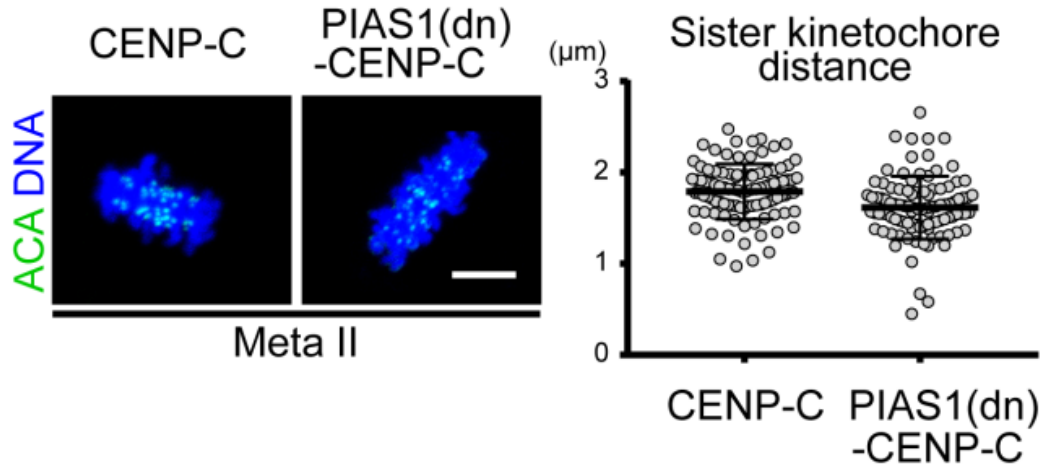

Fig. 35: Induction of PIAS1(dn)-CENP-C at MII egg does not cause cohesion defects. Metaphase II eggs expressing CENP-C or PIAS1(dn)-CENP-C were fixed 6 hr after mRNA injection. Centromeres (ACA, green) and chromosomes (Hoechst 33342, blue) were stained. Scale bar is 5 μm. Inter sister kinetochore distances were plotted (n=100, 100 from 5, 5 oocytes). (Ding *et al*, *Curr. Biol.* 2018)

3.9.2 Artificially activated centromeric sumoylation enhancement does not rescue cohesion defects in *Sgo2* knockout oocytes

Separase cleaves cohesins at anaphase I onset, and this activity might leak to post-anaphase-I periods. It is possible that centromeric sumoylation counteracts the residual separase activity during post-anaphase-I periods. If this is true, forced enhancement of centromeric sumoylation may have the capacity to rescue the cohesion defects at anaphase I onset in *Sgo2* knockout oocytes. To test this possibility, I expressed mNG-PIAS1-CENP-C in *Sgo2* knockout oocytes. I monitored the sister kinetochore distances at anaphase I onset, when separase activity reaches maximum. However, there was no significant difference of sister kinetochore distances in *Sgo2*

knockout oocytes expressing mNG-PIAS1-CENP-C or mNG-CENP-C (Fig. 36). Thus, artificially activated sumoylation enhancement at centromeres did not rescue the centromeric cohesion defects at anaphase I onset in *Sgo2* knockout oocytes. In summary, enhanced centromeric sumoylation is not sufficient to suppress separase activity.

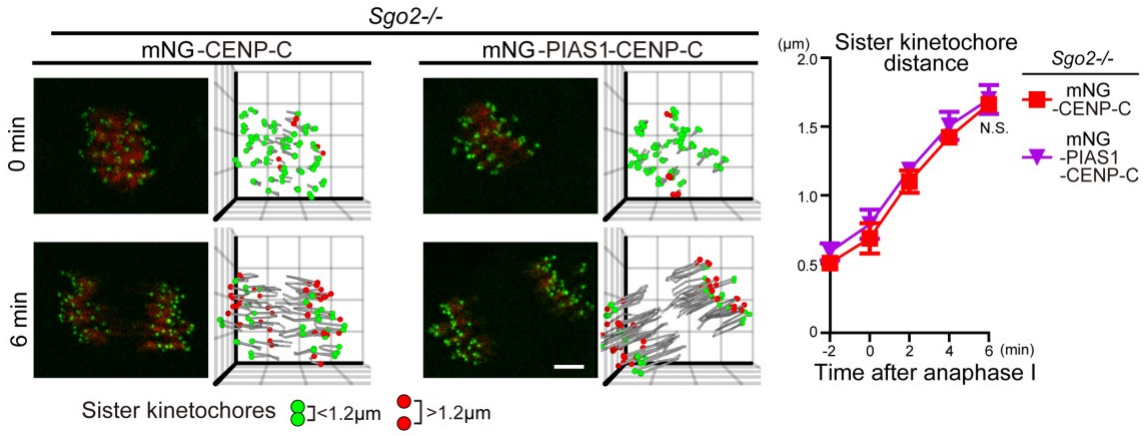

Fig. 36: Time-lapse imaging of *Sgo2*-/- oocytes expressing mNG-CENP-C or mNG-PIAS1-CENP-C (green) and H2B-mCherry (red). As a reference, *Sgo2*-/- oocytes expressing mNG-CENP-C is also shown. Kinetochore signal was enhanced and background was subtracted. Scale bar is 5 μm. The 3D plot shows the trajectory of the kinetochores (spheres). Sister kinetochores exhibiting >1.2 μm inter kinetochore distances are indicated by red spheres, while the others are indicated by green spheres. Inter sister kinetochore distances were also plotted over the time. (n= 3, 4 oocytes) Time after anaphase I onset (min). Error bars indicate SD. N.S. not significant. (Ding *et al*, *Curr. Biol.* 2018)

3.10 Enrichment of centromeric sumoylation at telophase is not specific to meiosis

I had shown that enhancement of centromeric sumoylation after anaphase I played a crucial role in centromeric cohesion maintenance in meiosis. However, in mitosis there is no need to maintain centromeric cohesion after anaphase, so I speculated that centromeric SUMO2/3 enrichment at telophase I was specific for meiosis I. To test this, I expressed mNG-SUMO2gg and H2B-mCherry at 1-cell stage zygotes and then monitored the first mitosis by live imaging. Similar to meiosis I, mNG-SUMO2gg showed nuclear signals at prophase, disappeared at metaphase, and stayed undetectable at anaphase. However, mNG-SUMO2gg signals also started to accumulate near centromeres at telophase, although it did not diminish from centromeres even after entering prophase of second mitosis (Fig. 37). In summary, enrichment of centromeric SUMO2/3 is not specific to meiosis.

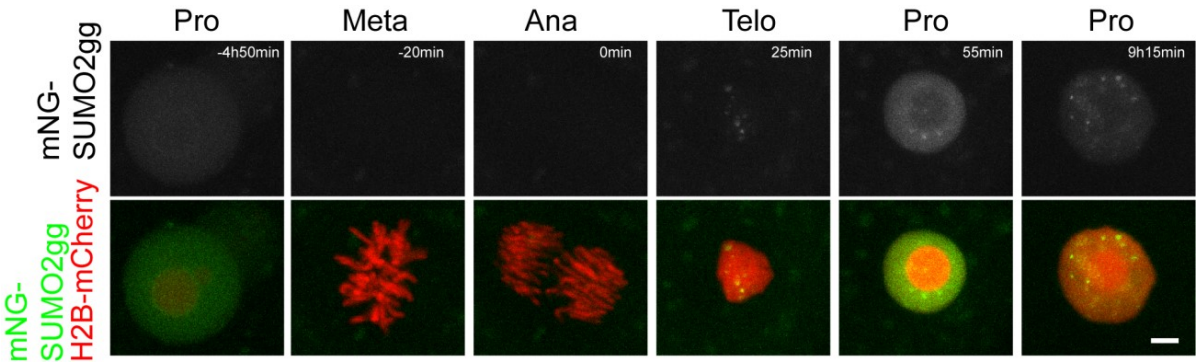

Fig. 37: mNG-SUMO2gg exhibits centromeric enrichment at telophase and persists until late prophase. One-cell stage zygotes expressing mNG-SUMO2gg (green) and H2B-mCherry (chromosomes, red) were imaged. Time after anaphase onset (min). Scale bar is 5 μm.

4. Discussions

SMT3 (suppressor of mif two 3 homolog 1), the SUMO ortholog in *S. cereviviae*, was first isolated as a high-copy suppressor of MIF2 mutations (Meluh & Koshland, 1995). Moreover, in vertebrate cells, SUMO1 was identified as a suppressor of CENP-C malfunction (Fukagawa et al, 2001). However, SUMO1 is dispensable for mouse embryonic development while SUMO2 is not (Wang et al, 2014), which raised the possibility that SUMO2/3 are capable to take over the functions of SUMO1 in meiosis. In this thesis, I showed that SUMO2/3 enrichment near centromeres depends on PIAS proteins, which are presumably recruited by CENP-C, so it is possible that PIAS proteins are the missing links of the compensation effect between CENP-C and SUMO. Moreover, the interaction between CENP-C and PIAS proteins might be conserved among eukaryotes.

I demonstrated that SUMO2/3 enrichment ensures cohesion protection during post-anaphase-I periods, whereas Sgo2 pathway acts at anaphase I onset. Considering that plant meiosis also needs a mechanism that follows shugoshin-dependent protection for the maintenance of centromeric cohesion throughout the meiosis I-II transition (Cromer et al, 2013), it is possible that the requirement of mechanisms that act at later stages of the meiosis I-II transition is also conserved.

The fact that PIAS1 and MEIKIN compete for the C-terminus of CENP-C in yeast three-hybrid assays also raises an interesting question about how PIAS proteins are regulated during meiosis. MEIKIN, which is critical for Sgo2 recruitment to centromeres, localizes at centromeres by anaphase I (Kim et al, 2015). In contrast, PIAS proteins and SUMO2/3 enrich near centromeres after anaphase I. Thus, it is possible that the dissociation of MEIKIN from kinetochores after the onset of anaphase I contributes to

the promotion of kinetochore recruitment of PIAS proteins by providing the binding sites of CENP-C for PIAS proteins. Although this notion is supported by evidence that tethering PIAS1 to centromeres decreases centromeric Sgo2 levels, it still needs further experiments to validate the competition mechanism for PIAS proteins regulation in meiosis.

Another important question is what centromeric sumoylation targets to protect centromeric cohesion during post-anaphase-I stages. Candidate proteins for sumoylation targets would include cohesin itself, cohesin remover and cohesin protector. The mitotic cohesin component Scc1 and the regulator Pds5 are known to be regulated through sumoylation in *S. cereviviae* (McAleenan et al, 2012; Wu et al, 2012; D'Ambrosio & Lavoie, 2014). In this thesis, I examined the possibility that SUMO-dependent cohesion protection during post-anaphase-I is mediated by counteracting Wapl or separase activity. The results are that Wapl pathway is less likely to get involved in SUMO-dependent cohesion protection pathway. Meanwhile, it is not conclusive whether centromeric sumoylation acts through opposing residual separase activity during post-anaphase-I stages. Nevertheless, there might be other cohesin removers involved in SUMO-dependent cohesion protection pathway. Future SUMO proteomics analysis during telophase I in meiosis will certainly lead to better understanding of SUMO-dependent cohesion protection pathway.

Insufficient centromeric sumoylation levels during post-anaphase I stages leads to precocious loss of centromeric cohesion, which raises a question whether centromeric sumoylation-dependent cohesion protection is defective after aging. It has already been proved that trisomy incidence dramatically increases as pregnancy age goes older

(Nagaoka et al, 2012). The cohesin complex is established at embryonic stage in mammals, and there is no turnover of cohesin for oocytes after decades of arresting at dictyotene stage (Tachibana-Konwalski et al, 2010). Instead, the cohesin complex undergoes a gradual decreasing during aging process, which is the leading cause of age related aneuploidy in oocytes (Chiang et al, 2010). Because cohesin protector Sgo2 decreases during aging (Lister et al, 2010), it will be not surprising that centromeric SUMO level also decays during aging. Thus, further studies of centromeric sumoylation-dependent cohesion maintenance during aging may shed light to better understanding of age related aneuploidy in oocytes.

5. References

Alonso A, Greenlee M, Matts J, Kline J, Davis KJ & Miller RK (2015) Emerging roles of sumoylation in the regulation of actin, microtubules, intermediate filaments, and septins. *Cytoskeleton (Hoboken, N.j.)* **72:** 305–339

Chiang T, Duncan FE, Schindler K, Schultz RM & Lampson MA (2010) Evidence that weakened centromere cohesion is a leading cause of age-related aneuploidy in oocytes. *Current biology : CB* **20:** 1522–1528

Corbett KD, Yip CK, Ee L-S, Walz T, Amon A & Harrison SC (2010) The monopolin complex cross-links kinetochore components to regulate chromosome-microtubule attachments. *Cell* **142:** 556–567

Cromer L, Jolivet S, Horlow C, Chelysheva L, Heyman J, Jaeger G de, Koncz C, Veylder L de & Mercier R (2013) Centromeric cohesion is protected twice at meiosis, by SHUGOSHINs at anaphase I and by PATRONUS at interkinesis. *Current biology : CB* **23:** 2090–2099

D'Ambrosio LM & Lavoie BD (2014) Pds5 prevents the PolySUMO-dependent separation of sister chromatids. *Current biology : CB* **24:** 361–371

Ding Y, Kaido M, Llano E, Pendas AM & Kitajima TS (2018) The Post-anaphase SUMO Pathway Ensures the Maintenance of Centromeric Cohesion through Meiosis I-II Transition in Mammalian Oocytes. *Current biology : CB*

Eifler K, Cuijpers SAG, Willemstein E, Raaijmakers JA, El Atmioui D, Ovaa H, Medema RH & Vertegaal ACO (2018) SUMO targets the APC/C to regulate transition from metaphase to anaphase. *Nature communications* **9:** 1119

Feitosa WB, Hwang K & Morris PL (2018) Temporal and SUMO-specific SUMOylation contribute to the dynamics of Polo-like kinase 1 (PLK1) and spindle integrity during mouse oocyte meiosis. *Developmental biology* **434:** 278–291

Fukagawa T, Regnier V & Ikemura T (2001) Creation and characterization of temperature-sensitive CENP-C mutants in vertebrate cells. *Nucleic Acids Research* **29:** 3796–3803

Gandhi R, Gillespie PJ & Hirano T (2006) Human Wapl is a cohesin-binding protein that promotes sister-chromatid resolution in mitotic prophase. *Current biology : CB* **16:** 2406–2417

Gietz RD & Schiestl RH (2007) High-efficiency yeast transformation using the LiAc/SS carrier DNA/PEG method. *Nature protocols* **2:** 31–34

Haarhuis JHI, Elbatsh AMO & Rowland BD (2014) Cohesin and its regulation: on the logic of X-shaped chromosomes. *Developmental cell* **31:** 7–18

Hauf S (2001) Cohesin Cleavage by Separase Required for Anaphase and Cytokinesis in Human Cells. *Science (New York, N.Y.)* **293:** 1320–1323

Hay RT (2005) SUMO: a history of modification. *Molecular cell* **18:** 1–12

Huang C-J, Di Wu, Khan FA & Huo L-J (2015) The SUMO Protease SENP3 Orchestrates G2-M Transition and Spindle Assembly in Mouse Oocytes. *Scientific reports* **5:** 15600

Huang J & Moazed D (2006) Sister chromatid cohesion in silent chromatin: each sister to her own ring. *Genes & development* **20:** 132–137

Ishiguro K-I, Kim J, Fujiyama-Nakamura S, Kato S & Watanabe Y (2011) A new meiosis-specific cohesin complex implicated in the cohesin code for homologous pairing. *EMBO reports* **12:** 267–275

Ishiguro T, Tanaka K, Sakuno T & Watanabe Y (2010) Shugoshin-PP2A counteracts casein-kinase-1-dependent cleavage of Rec8 by separase. *Nature cell biology* **12:** 500–506

Katis VL, Lipp JJ, Imre R, Bogdanova A, Okaz E, Habermann B, Mechtler K, Nasmyth K & Zachariae W (2010) Rec8 Phosphorylation by Casein Kinase 1 and Cdc7-Dbf4 Kinase Regulates Cohesin Cleavage by Separase during Meiosis. *Developmental cell* **18:** 397–409

Kerrebrock AW, Moore DP, Wu JS & Orr-Weaver TL (1995) Mei-S332, a Drosophila protein required for sister-chromatid cohesion, can localize to meiotic centromere regions. *Cell* **83:** 247–256

Kim J, Ishiguro K-I, Nambu A, Akiyoshi B, Yokobayashi S, Kagami A, Ishiguro T, Pendas AM, Takeda N, Sakakibara Y, Kitajima TS, Tanno Y, Sakuno T & Watanabe Y (2015) Meikin is a conserved regulator of meiosis-I-specific kinetochore function. *Nature* **517:** 466–471

Kim YS, Nagy K, Keyser S & Schneekloth JS (2013) An electrophoretic mobility shift assay identifies a mechanistically unique inhibitor of protein sumoylation. *Chemistry & biology* **20:** 604–613

Kitajima TS, Kawashima SA & Watanabe Y (2004) The conserved kinetochore protein shugoshin protects centromeric cohesion during meiosis. *Nature* **427:** 510–517

Kitajima TS, Ohsugi M & Ellenberg J (2011) Complete kinetochore tracking reveals error-prone homologous chromosome biorientation in mammalian oocytes. *Cell* **146:** 568–581

Klapholz S & Esposito RE (1980) Isolation of SPO12–1 and SPO13–1 from a Natural Variant of Yeast That Undergoes a Single Meiotic Division. *Genetics* **96:** 567–588

Klein F, Mahr P, Galova M, Buonomo SB, Michaelis C, Nairz K & Nasmyth K (1999) A central role for cohesins in sister chromatid cohesion, formation of axial elements, and recombination during yeast meiosis. *Cell* **98:** 91–103

Kudo NR, Anger M, Peters AHFM, Stemmann O, Theussl H-C, Helmhart W, Kudo H, Heyting C & Nasmyth K (2009) Role of cleavage by separase of the Rec8 kleisin subunit of cohesin during mammalian meiosis I. *Journal of cell science* **122:** 2686–2698

Kueng S, Hegemann B, Peters BH, Lipp JJ, Schleiffer A, Mechtler K & Peters J-M (2006) Wapl controls the dynamic association of cohesin with chromatin. *Cell* **127:** 955–967

Lee J, Kitajima TS, Tanno Y, Yoshida K, Morita T, Miyano T, Miyake M & Watanabe Y (2008) Unified mode of centromeric protection by shugoshin in mammalian oocytes and somatic cells. *Nature cell biology* **10:** 42–52

Liang M, Melchior F, Feng X-H & Lin X (2004) Regulation of Smad4 sumoylation and transforming growth factor-beta signaling by protein inhibitor of activated STAT1. *The Journal of biological chemistry* **279:** 22857–22865

Lister LM, Kouznetsova A, Hyslop LA, Kalleas D, Pace SL, Barel JC, Nathan A, Floros V, Adelfalk C, Watanabe Y, Jessberger R, Kirkwood TB, Höög C & Herbert M (2010) Age-related meiotic segregation errors in mammalian oocytes are preceded by depletion of cohesin and Sgo2. *Current biology : CB* **20:** 1511–1521

Liu H, Rankin S & Yu H (2012) Phosphorylation-enabled binding of Sgo1–PP2A to cohesin protects sororin and centromeric cohesion during mitosis. *Nature cell biology* **15:** 40–49

Llano E, Gómez R, Gutiérrez-Caballero C, Herrán Y, Sánchez-Martín M, Vázquez-Quiñones L, Hernández T, Alava E de, Cuadrado A, Barbero JL, Suja JA & Pendás AM (2008) Shugoshin-2 is essential for the completion of meiosis but not for mitotic cell division in mice. *Genes & development* **22:** 2400–2413

McAleenan A, Cordon-Preciado V, Clemente-Blanco A, Liu I-C, Sen N, Leonard J, Jarmuz A & Aragón L (2012) SUMOylation of the α-kleisin subunit of cohesin is required for DNA damage-induced cohesion. *Current biology : CB* **22:** 1564–1575

Meluh PB & Koshland D (1995) Evidence that the MIF2 gene of Saccharomyces cerevisiae encodes a centromere protein with homology to the mammalian centromere protein CENP-C. *MBoC* **6:** 793–807

Nagaoka SI, Hassold TJ & Hunt PA (2012) Human aneuploidy: mechanisms and new insights into an age-old problem. *Nature reviews. Genetics* **13:** 493–504

O'Rourke JG, Gareau JR, Ochaba J, Song W, Raskó T, Reverter D, Lee J, Monteys AM, Pallos J, Mee L, Vashishtha M, Apostol BL, Nicholson TP, Illes K, Zhu Y-Z, Dasso M, Bates GP, Difiglia M, Davidson B & Wanker EE et al (2013) SUMO-2 and PIAS1 Modulate Insoluble Mutant Huntingtin Protein Accumulation. *Cell reports* **4:** 362–375

Pelisch F, Sonneville R, Pourkarimi E, Agostinho A, Blow JJ, Gartner A & Hay RT (2014) Dynamic SUMO modification regulates mitotic chromosome assembly and cell cycle progression in Caenorhabditis elegans. *Nature communications* **5:** 5485

Pelisch F, Tammsalu T, Wang B, Jaffray EG, Gartner A & Hay RT (2017) A SUMO-Dependent Protein Network Regulates Chromosome Congression during Oocyte Meiosis. *Molecular cell* **65:** 66–77

Prasada Rao HBD, Qiao H, Bhatt SK, Bailey LRJ, Tran HD, Bourne SL, Qiu W, Deshpande A, Sharma AN, Beebout CJ, Pezza RJ & Hunter N (2017) A SUMO-ubiquitin relay recruits

proteasomes to chromosome axes to regulate meiotic recombination. *Science (New York, N.Y.)* **355:** 403–407

Rabut G & Ellenberg J (2004) Automatic real-time three-dimensional cell tracking by fluorescence microscopy. *Journal of microscopy* **216:** 131–137

Revenkova E, Eijpe M, Heyting C, Hodges CA, Hunt PA, Liebe B, Scherthan H & Jessberger R (2004) Cohesin SMC1β is required for meiotic chromosome dynamics, sister chromatid cohesion and DNA recombination. *Nature cell biology* **6:** 555–562

Sakakibara Y, Hashimoto S, Nakaoka Y, Kouznetsova A, Höög C & Kitajima TS (2015) Bivalent separation into univalents precedes age-related meiosis I errors in oocytes. *Nature communications* **6:** 7550

Sambrook J, Fritsch EF & Maniatis T (1989) *Molecular cloning.* Cold Spring Harbor Laboratory Press, Cold Spring Harbor, N.Y.

Schindelin J, Arganda-Carreras I, Frise E, Kaynig V, Longair M, Pietzsch T, Preibisch S, Rueden C, Saalfeld S, Schmid B, Tinevez J-Y, White DJ, Hartenstein V, Eliceiri K, Tomancak P & Cardona A (2012) Fiji: an open-source platform for biological-image analysis. *Nature methods* **9:** 676–682

Shindo N, Kumada K & Hirota T (2012) Separase sensor reveals dual roles for separase coordinating cohesin cleavage and cdk1 inhibition. *Developmental cell* **23:** 112–123

Tachibana-Konwalski K, Godwin J, van der Weyden L, Champion L, Kudo NR, Adams DJ & Nasmyth K (2010) Rec8-containing cohesin maintains bivalents without turnover during the growing phase of mouse oocytes. *Genes & development* **24:** 2505–2516

Tanaka K, Chang HL, Kagami A & Watanabe Y (2009) CENP-C functions as a scaffold for effectors with essential kinetochore functions in mitosis and meiosis. *Developmental cell* **17:** 334–343

Tanenbaum ME, Gilbert LA, Qi LS, Weissman JS & Vale RD (2014) A protein-tagging system for signal amplification in gene expression and fluorescence imaging. *Cell* **159:** 635–646

Tanno Y, Kitajima TS, Honda T, Ando Y, Ishiguro K-I & Watanabe Y (2010) Phosphorylation of mammalian Sgo2 by Aurora B recruits PP2A and MCAK to centromeres. *Genes & development* **24:** 2169–2179

Unhavaithaya Y & Orr-Weaver TL (2013) Centromere proteins CENP-C and CAL1 functionally interact in meiosis for centromere clustering, pairing, and chromosome segregation. *Proceedings of the National Academy of Sciences of the United States of America* **110:** 19878–19883

Wang L, Wansleeben C, Zhao S, Miao P, Paschen W & Yang W (2014) SUMO2 is essential while SUMO3 is dispensable for mouse embryonic development. *EMBO reports* **15:** 878–885

Wang Z-B, Ou X-H, Tong J-S, Li S, Wei L, Ouyang Y-C, Hou Y, Schatten H & Sun Q-Y (2010) The SUMO pathway functions in mouse oocyte maturation. *Cell Cycle* **9:** 2640–2646

Watanabe Y & Nurse P (1999) Cohesin Rec8 is required for reductional chromosome segregation at meiosis. *Nature* **400:** 461–464

Wu N, Kong X, Ji Z, Zeng W, Potts PR, Yokomori K & Yu H (2012) Scc1 sumoylation by Mms21 promotes sister chromatid recombination through counteracting Wapl. *Genes & development* **26:** 1473–1485

Yokobayashi S & Watanabe Y (2005) The kinetochore protein Moa1 enables cohesion-mediated monopolar attachment at meiosis I. *Cell* **123:** 803–817

Yoshida S, Kaido M & Kitajima TS (2015) Inherent Instability of Correct Kinetochore-Microtubule Attachments during Meiosis I in Oocytes. *Developmental cell* **33:** 589–602

Yuan Y-F, Zhai R, Liu X-M, Khan HA, Zhen Y-H & Huo L-J (2014) SUMO-1 plays crucial roles for spindle organization, chromosome congression, and chromosome segregation during mouse oocyte meiotic maturation. *Molecular reproduction and development* **81:** 712–724

Yurchenko V, Xue Z & Sadofsky MJ (2006) SUMO modification of human XRCC4 regulates its localization and function in DNA double-strand break repair. *Molecular and cellular biology* **26:** 1786–1794

Zhang X-D, Goeres J, Zhang H, Yen TJ, Porter ACG & Matunis MJ (2008) SUMO-2/3 modification and binding regulate the association of CENP-E with kinetochores and progression through mitosis. *Molecular cell* **29:** 729–741

Acknowledgment

Many people have helped during my PhD career; I really appreciate their kind advice during my PhD course.

I thank my supervisor Dr. Tomoya Kitajima, who mentored me and endure my slow progress. My PhD career would not have been possible without the financial supports from MEXT scholarship from Japanese Government. I would also thank Dr. Fumio Matsuzaki and Dr. Tomohiro Matsumoto as my sub-supervisor; they really helped a lot to improve my research career. I would also thank Dr. Masako Kaido for Y2H screening; Drs. J. Kim and Y. Watanabe for technical assistance, providing the Sgo2 antibody, and transferring *Sgo2*-/- mice; J. Ellenberg for the macro for automated microscopy; the imaging, animal, and genome resource and analysis facilities of RIKEN BDR for support. I really appreciate my laboratory members, Drs. Aurelien Courtois, Shuhei Yoshida, Hirohisa Kyogoku for kind discussion and help on experiments.

This thesis is based on the following paper:

Ding et al., The Post-anaphase SUMO Pathway Ensures the Maintenance of Centromeric Cohesion through Meiosis I-II Transition in Mammalian Oocytes, *Current Biology* (2018), 28, 1661-1669.